https://doi.org/10.5194/egusphere-2026-3352
Preprint. Discussion started: 7 July 2026
© Author(s) 2026. CC BY 4.0 License.

Development and comparison of documentary-instrumental and circulation-based multi-centennial precipitation reconstructions for Dublin, Ireland

Csaba Horvath[1], Conor Murphy[1], Ciara Ryan[2]

[1] *Irish Climate Analysis and Research Units (ICARUS), Dept. of Geography, Maynooth University, Co. Kildare, Ireland.*

[2] *Climate Services Division, Met Éireann, Dublin, Ireland.*

Correspondence to: Csaba Horvath (csaba.horvath.2023@mumail.ie)

Abstract

This study develops a multi-centennial reconstruction of precipitation for the Greater Dublin Area, Ireland, using documentary, instrumental, circulation-based, and proxy evidence. Three independent reconstructions are produced for two contrasting water-resource domains, including: a monthly scaled version of the Jenkinson documentary-instrumental rainfall dataset for 1711-1977 produced by an earlier analysis for the island of Ireland; a circulation-informed monthly statistical ensemble based on Lasso and Random Forest models for 1748-1994; and an annual oak cellulose $\delta^{18}O$ reconstruction of May-August precipitation extending to 1200 CE. Reconstructions were assessed against 1 km gridded rainfall observations for the common overlap period 1865-1977 using correlation, bias, error metrics, SPI-based event detection, and agreement in ranked wet and dry extremes. Long-term UK rainfall series and an extended Dublin snow and sleet series were used as independent comparators. Both the Jenkinson and statistical ensemble reconstructions reproduce observed monthly, seasonal, and annual rainfall variability, but the Jenkinson reconstruction shows the strongest agreement across most metrics and better captures wet and dry extremes. The statistical ensemble provides an independent, physically interpretable reconstruction, although it tends to smooth variability and under-represent event magnitude. The $\delta^{18}O$ reconstruction shows weaker interannual agreement with observed May-August rainfall but provides a valuable longer-term perspective on summer hydroclimatic variability. Divergence between the Jenkinson and ensemble reconstructions before the mid-nineteenth century, particularly in winter and spring, is consistent with possible snow- and sleet-related undercatch in early precipitation sources which affects the Jenkinson reconstruction. Summer rainfall during the eighteenth century remains uncertain, with evidence for increased regional hydroclimatic heterogeneity. Together, these reconstructions provide a

https://doi.org/10.5194/egusphere-2026-3352
Preprint. Discussion started: 7 July 2026
© Author(s) 2026. CC BY 4.0 License.

stronger basis for contextualising historical droughts and pluvials affecting Dublin and for stress-testing water-resource systems beyond the instrumental period.

Keywords (7): Historical climatology; Precipitation reconstruction; Documentary evidence; Tree-ring $\delta^{18}O$; Data rescue; Water resources; Greater Dublin Area

1. Introduction

Long-term rainfall reconstructions are fundamental to water resource management, offering the possibility of extending the evidence base for yield assessments, drought planning, and decision-making beyond the instrumental period. They can also provide the context needed to distinguish emerging anthropogenic change from climate variability (Fordham and Murphy, 2026) and identify historically plausible drought and wet periods for stress testing infrastructure and management plans (Noone et al., 2017; Wilby et al., 2015; Wilby and Murphy, 2019) Historical climatology and palaeoclimatology consistently demonstrate that hydroclimatic variability inferred from the instrumental era alone can underestimate both the severity and persistence of extremes, with direct implications for water-supply reliability, infrastructure design, and climate adaptation planning (Wetter et al., 2014; Cook et al., 2015; Blöschl et al., 2020; Brázdil et al., 2020a; Büntgen et al., 2021). Beyond water resource management, Engler et al. (2013) show how precipitation reconstructions can shed light on previous extremes, such as the 1740-41 famine in Ireland, while Murphy et al. (2020) highlight the extent of multi-annual drought across the British and Irish Isles in 1765. Jobbová et al. (2024) have linked precipitation reconstructions with newspaper records to examine drought impacts in Ireland from the early 1700s to the present.

Ireland has a rich history of weather observing, with systematic observations beginning in Dublin in 1789 (Shields, 1983). Recent research has attempted to leverage these data, with Noone et al. (2016) developing a homogenised network of 25 long-term monthly precipitation gauges across the island from 1850 onwards, and Ryan et al. (2022) developing a network of long-term daily stations extending back to the late 1800s. Others, including Jenkinson et al. (1979) and Murphy et al. (2018), have also used observations and documentary sources to develop a monthly rainfall series for the Island of Ireland from 1711 to the present.

In addition to these observations, Murphy et al. (2020) have used circulation-based predictors to reconstruct monthly precipitation totals for regional precipitation series across the British

https://doi.org/10.5194/egusphere-2026-3352
Preprint. Discussion started: 7 July 2026
© Author(s) 2026. CC BY 4.0 License.

and Irish Isles using multiple linear regression. In addition to extending available regional series for the Island of Ireland, Scotland and the England and Wales Precipitation (EWP) series to 1748, Murphy et al. (2020) used circulation-informed precipitation reconstructions to show that winter totals in the EWP series may be underestimated given changes in gauge design and undercatch of snow prior to circa 1860. At a European scale, Pauling et al. (2006) developed seasonal gridded precipitation fields for land areas at 0.5° x 0.5° resolution from 1500-1900 using principal component regression combining long instrumental precipitation series, documentary information and natural proxies, including tree rings, ice cores, corals and speleothems as predictors. Reconstruction skill over Ireland is good for all seasons from circa 1700 onwards, with the data previously used as a benchmark against which other Irish reconstructions have been assessed (Murphy et al., 2018). Relatedly, Casty et al. (2007) also provide reconstructions of monthly precipitation from 1766 onwards, which have previously been employed, following bias correction, to extend river flow reconstructions for 51 Irish catchments (O'Connor et al., 2021).

While these datasets and reconstructions have been very valuable for assessing of past extremes, they are often not configured around the spatial units relevant to water-resource planning and may not fully capture important local heterogeneity in precipitation variability. Recent data rescue initiatives, including Rainfall Rescue (Hawkins et al., 2023) and transcription of historical Irish rain-gauge records by Met Éireann (Ireland's national meteorological service, Ryan et al., 2021; Ryan and McGovern, 2025), have substantially strengthened the observational basis for long-term rainfall assessment and increased potential for developing bespoke multi-century reconstructions for key water resource zones. Despite Ireland's generally wet climate, the Greater Dublin Area, which encompasses Ireland's largest metropolitan region, is highly vulnerable to drought. This vulnerability reflects the combination of high and growing water demand, ageing infrastructure with little spare capacity, relatively low rainfall compared to western Ireland, limited local storage, strong dependence on key surface-water sources, and sensitivity to seasonal rainfall deficits (Kelly-Quinn et al., 2014).

This study reconstructs monthly precipitation for two water resource zones in the GDA using three approaches: (i) month-specific statistical reconstructions (Lasso and random-forest regression) driven by circulation and hydroclimate predictors (back to 1748), (ii) scaling of a rainfall anomaly dataset compiled by Jenkinson et al. (1979) (back to 1711), and (iii) an annually resolved oak cellulose $\delta^{18}O$ proxy chronology, developed for Central England (Loader et al., 2019) and used here to reconstruct growing-season precipitation (MJJA) back to 1200.

https://doi.org/10.5194/egusphere-2026-3352
Preprint. Discussion started: 7 July 2026
© Author(s) 2026. CC BY 4.0 License.

The key aims of this work are to i) leverage available datasets to produce multi-centennial reconstructions of monthly precipitation that water managers can use to evaluate historical extremes (both drought and pluvials), and ii) examine how skilfully different approaches to reconstruction can capture precipitation variability and extremes across contrasting upland and lowland domains within the GDA. The remainder of the paper is structured as follows. Section 2 describes the study area, datasets, reconstruction methods, and the evaluation approaches used to assess performance. Section 3 presents the reconstruction results, including calibration/validation and comparative analysis over the observational overlap period. Section 4 discusses the utility and limitations of each reconstruction approach and key insights from reconstructions. Section 5 concludes with the main findings and implications.

2. Study Area, Data and Methods

2.1 Study Area

The Greater Dublin Area (GDA) in eastern Ireland spans lowland coastal terrain and the adjacent Wicklow Mountains, producing sharp rainfall gradients over short distances. Ireland's water-resources planning framework is structured around Regional Water Resources Plans (RWRPs), which subdivide Regional Water Management Areas into Study Areas (SAs) comprising one or more Water Resource Zones (WRZs). The GDA broadly aligns with Uisce Éireann's (Ireland's national water utility; formerly Irish Water) Study Areas SA1, SA2 and SA9. SA1 and SA2 are upland areas in County Wicklow, covering the eastern and western halves of the northern Wicklow Mountains, and include small settlements and headwater catchments. SA9 is predominantly urban and spans County Dublin and parts of adjacent counties, with a population of approximately 1.7 million. The GDA supply system serves a great, spatially concentrated demand and is substantially reliant on the River Liffey, increasing sensitivity to prolonged rainfall deficits and operational shocks (Uisce Éireann, 2022a, 2022b). For precipitation reconstruction, SA9 is retained as defined by Uisce Éireann, while SA1 and SA2 are combined into a single upland domain (hereafter SA-upland) to reflect hydrological similarity (Figure 1). Reconstructions are produced and evaluated separately for SA9 and SA-upland and evaluated against gridded observational rainfall.

https://doi.org/10.5194/egusphere-2026-3352
Preprint. Discussion started: 7 July 2026
© Author(s) 2026. CC BY 4.0 License.

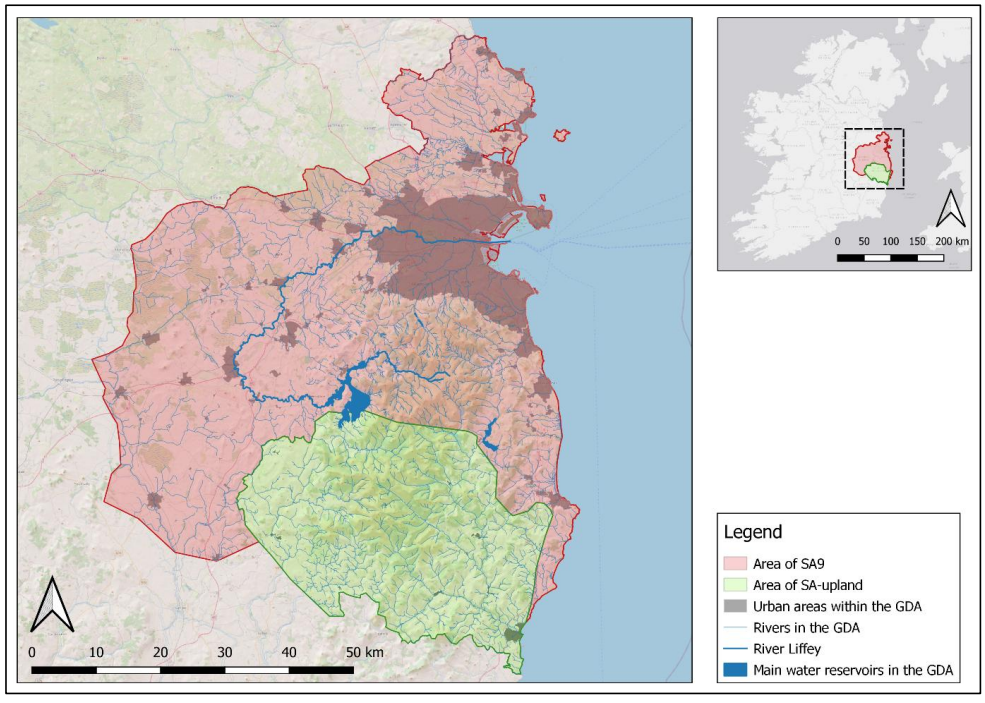

Figure 1 Map of the Greater Dublin Area (GDA) on the east coast of Ireland. The GDA is defined here as the combination of Uisce Éireann water management areas SA9 (red shading) and the merged SA1-SA2 regions, referred to in the study as "SA upland" (green shading). Grey shading denotes urban areas within the GDA, whereas blue indicates water bodies, including the River Liffey (highlighted by the thicker blue line) and the main reservoirs supplying the Dublin region. Source: the map is the author's work in QGIS

2.2 Data

2.2.1 Observed gridded rainfall dataset (1865-2024)

Observed monthly precipitation is represented using a 1 km gridded rainfall dataset (1865-2024) produced by Met Éireann. Inputs are drawn mainly from the modern station network after 1941, while earlier decades incorporate extensive rescued historical gauge data, including Rainfall Rescue digitisation (Hawkins et al., 2023) and additional Met Éireann transcriptions (Ryan et al., 2021; Ryan and McGovern, 2025). Grids are generated using regression on physiographic predictors and kriged residuals, and evaluated by cross-validation, providing an internally consistent reference for comparison with reconstructions (Coonan et al., 2024). The product is provided on the Irish National Grid (TM75/Irish Grid; EPSG:29903). A single series of monthly totals for each domain was extracted from the gridded data for use in subsequent analysis. As with all long-term gridded gauge-based precipitation products, station density and

https://doi.org/10.5194/egusphere-2026-3352
Preprint. Discussion started: 7 July 2026
© Author(s) 2026. CC BY 4.0 License.

record continuity are generally lower in complex terrain and in earlier periods (Hofstra et al., 2009; Newman et al., 2015; Cornes et al., 2018). Interpolation can smooth small-scale variability and dampen local extremes relative to point observations, but it may introduce larger uncertainties in upland areas where rainfall gradients are strong (Daly 2006; Hofstra et al., 2009; Herrera et al., 2012; Daly et al., 2021; Matiu et al., 2024). Finally, gridded totals inherit known gauge-measurement biases - particularly exposure, wind and snow-induced undercatch (Adam and Lettenmaier, 2003; Murphy et al., 2018; Pollock et al., 2018; Hawkins et al., 2023; Kendon et al., 2023).

2.2.2 The Jenkinson Dataset (1711-1977)

The Jenkinson dataset is a documentary-instrumental rainfall series for the island of Ireland derived from an unpublished UK Meteorological Office note compiled by Jenkinson et al. (1979). It provides continuous Ireland-wide monthly rainfall estimates for 1711-1977, expressed as (i) annual rainfall anomalies (annual totals expressed as a percentage of an estimated annual average rainfall, AAR) and (ii) proportional monthly rainfall distributions expressed as 'internal percentages' of the annual total. While Jenkinson et al (1979) provide an island-wide series, resampling AAR for the GDA allows the annual anomaly and monthly distribution information to be re-anchored to the rainfall climatology for the Dublin domains considered here.

It is important to note that the Jenkinson series draws on a changing mixture of source materials through time, including early rain-gauge observations, documentary weather diaries, regional UK rainfall series used as proxy stations, and later Irish station observations. The full Jenkinson series, its compilation and its provenance are described in detail by Murphy et al. (2018). For much of the eighteenth century, the series is strongly informed by Rutty's Dublin weather diary (Rutty, 1770). From 1792-1839, observed Dublin rainfall data reported by Dixon (1953) are included, while monthly and annual totals for Dublin derived from the UK Met Office are also noted for 1823-1824. From 1840-1977, the series increasingly draws on monthly and annual totals from available long-term stations, including Dublin. For the mid- to late-twentieth century, inputs include long-term station data, including Dublin stations reported by Tabony (1980), monthly and annual totals from the Irish Meteorological Service/Met Éireann, and annual rainfall maps.

https://doi.org/10.5194/egusphere-2026-3352
Preprint. Discussion started: 7 July 2026
© Author(s) 2026. CC BY 4.0 License.

The Jenkinson series is therefore unlikely to be fully independent of the gridded observational rainfall dataset used for evaluation in this study, particularly during periods when both products may draw on early Dublin-area and Irish station observations, either directly or indirectly. For this reason, comparisons between the Jenkinson-based Dublin reconstruction and the gridded rainfall reference are interpreted as assessments of overlap-period agreement or consistency, rather than as fully independent validation. Nevertheless, the Jenkinson series provides a valuable long-term documentary-instrumental estimate of monthly precipitation variability. In this study, we refer to the Dublin-domain product as a Jenkinson-based reconstruction, because the original island-wide anomaly and monthly distribution information are re-anchored to domain-specific AAR estimates for SA9 and SA-upland.

2.2.3 Predictors used for statistical reconstructions (1748-1994)

Plausible predictors with potential utility for reconstructing monthly precipitation were compiled to develop statistical reconstruction approaches. The predictor set comprises quality-assured sea-level pressure (SLP) datasets, North Atlantic/European circulation indices, and auxiliary hydroclimate covariates, including Central England Temperature (CET), a monthly UK precipitation series, and the summer Palmer Drought Severity Index (PDSI) derived from the Old World Drought Atlas (Cook et al., 2015). All predictors used, their sources, and temporal coverage are summarised in Table 1. Reconstructions were undertaken from 1748 to1994 given the overlap of available predictors.

https://doi.org/10.5194/egusphere-2026-3352
Preprint. Discussion started: 7 July 2026
© Author(s) 2026. CC BY 4.0 License.

Series name (abbreviation used)	Source/reference	Why a plausible predictor
London sea-level pressure (LSLP)	*Cornes et al. (2012a,b)*	Represents synoptic-scale pressure variability that controls airflow and storm tracks affecting rainfall.
Dublin sea-level pressure (DSLP)	*Jones et al. (1987; 1999)*	Local pressure variability is directly linked to circulation regimes associated with wet/dry conditions.
Paris-London index (SLP gradient) (PL)	*Cornes et al. (2013)*	Proxy for zonal flow strength; stronger westerlies enhance moisture transport and rainfall.
SLP gridpoint near Dublin (grid 50) (g50)	*Casty et al. (2007)*	Captures regional-to-large-scale pressure variability influencing Irish rainfall at the monthly scale.
North Atlantic Oscillation index (variant 1) (nao1)	*Luterbacher et al. (2002)*	Key mode of North Atlantic circulation; modulates westerlies and storminess relevant to rainfall.
North Atlantic Oscillation index (variant 2) (nao2)	*Jones et al. (1997)*	The alternative NAO definition provides robustness; NAO is strongly linked to circulation-driven rainfall variability.
Hurrell NAO index (hu)	*Hurrell (1995)*	Basin-scale pressure contrast controls westerly flow and moisture advection into NW Europe.
Jones NAO index (j)	*Jones et al. (1997)*	Independent NAO variant; helps capture NAO-related circulation effects on rainfall.
Rogers NAO index (r)	*Rogers (1984)*	NAO-related circulation metric; linked to storm-track shifts influencing rainfall totals.
European circulation mode 1 (eu1)	*Barnston & Livezey (1987); Luterbacher et al. (1999);*	Represents Euro-Atlantic circulation regimes that modulate regional precipitation patterns.
European circulation mode 2 (eu2)	*Barnston & Livezey (1987); Luterbacher et al. (1999);*	Associated with blocking/zonal flow differences that influence rainfall occurrence and persistence.
Central England Temperature (CET)	*Manley (1974); Parker et al. (1992)*	Temperature covaries with circulation/airmass state and seasonality, which also influence rainfall regimes.
UK precipitation series (uk)	*Todd et al. (2013); Murphy et al. (2018)*	Nearby precipitation integrates similar synoptic forcing and provides a physically consistent hydroclimate constraint.
Old World Drought Atlas scPDSI (OWDA scPDSI)	*Cook et al. (2015)*	The hydroclimate index reflects moisture-balance variability that can covary with large-scale circulation and thereby affect rainfall.

Table 1 The monthly predictor suite used in circulation-based statistical reconstructions. All series are extracted for the maximum overlap period of 1748-1994.

https://doi.org/10.5194/egusphere-2026-3352
Preprint. Discussion started: 7 July 2026
© Author(s) 2026. CC BY 4.0 License.

2.2.4 Oxygen-isotope proxy data (tree-ring cellulose $\delta^{18}O$) (1200-2000)

This study uses tree-ring oxygen isotope ($\delta^{18}O$) data from the master chronology compiled by Loader et al. (2019) for Central England, spanning 1200-2000 CE, based on $\delta^{18}O$ measurements of oak tree-ring cellulose, to derive an annually resolved reconstruction of MJJA (May-August) precipitation variability. We use this dataset to provide an annually resolved proxy archive of growing-season hydroclimate variability from the wider British-Irish Isles region. Here, it is used to derive a May-August (MJJA) precipitation reconstruction for the Dublin rainfall domains by calibrating against observed MJJA rainfall during the instrumental overlap period. The purpose of including the $\delta^{18}O$-based reconstruction is therefore twofold: first, to provide an independent proxy-based comparison for summer hydroclimate variability during the period of overlap with gridded observations and the documentary-instrumental reconstructions; and second, to extend the assessment of regional summer hydroclimatic variability beyond the documentary-instrumental window. Its interpretation is restricted to MJJA rainfall variability and the longer-term summer hydroclimate context. It is not treated as a monthly reconstruction, nor as a direct local rainfall measurement for Dublin.

2.2.5 Long-term comparative series

Eastern Ireland and much of the UK lie within a common North Atlantic circulation domain, where precipitation variability at monthly to seasonal scales is modulated by large-scale modes such as the North Atlantic Oscillation and associated moisture-transport regimes (Wilby et al., 1997; Parry et al., 2023). As a result, long-term precipitation series from the UK can exhibit coherent variability with eastern Ireland and provide useful hydroclimatic context for interpreting reconstructed rainfall variability, particularly prior to the start of the Irish instrumental record. Four long-term UK monthly precipitation series were employed, including records from Kew Gardens (southern England), the Spalding/Pode Hole composite series (East Midlands), alongside two additional long-duration series from Carlisle (northwest England) and Oxford (south-central England). These series extend into the eighteenth century and are derived from combinations of early instrumental observations and documentary-based reconstructions, with varying degrees of uncertainty in their earliest segments (Wales-Smith, 1971; Craddock and Wales-Smith, 1977; Tabony, 1980; Todd et al., 2013; Murphy et al., 2018). In addition, we compare seasonal totals from our reconstructions with those of Pauling et al.

https://doi.org/10.5194/egusphere-2026-3352
Preprint. Discussion started: 7 July 2026
© Author(s) 2026. CC BY 4.0 License.

(2006). This comparison is limited to SA9 for the period 1700-2000, as the grid resolution of the Pauling et al. dataset does not allow for the adequate representation of SA_upland. Seasonal totals from Pauling et al. were extracted for two grids overlapping SA9 and a regional average derived across both cells. Together, these series provide independent benchmarks against which the timing, persistence, and relative magnitude of reconstructed wet and dry periods can be assessed.

2.2.6 Dublin snow and sleet series (DSS) and Manley (MSS) snow and sleet series

To assess whether early winter rainfall measurements may be biased low because of undercatch of snow or mixed precipitation (Murphy et al., 2019), we use the Dublin snow and sleet dataset (DSS) developed for the GDA (Horvath et al., 2025). DSS summarises the number of days with snow and/or sleet at monthly, seasonal (October-May) and annual scales for 1867-2024, based on six long-running observing sites across the GDA, and is published as an aggregated regional series. Here, DSS is used as an independent indicator of precipitation phase. For analyses requiring longer temporal coverage, DSS is extended back to 1748 using the London snow and sleet series compiled by Gordon Manley (1969), which was subsequently digitised and extended to 1974 (Murphy et al., 2019). The Manley series is based on a synthesis of early instrumental observations and documentary evidence from the greater London area and provides one of the longest continuous records of snowfall and sleet occurrence in the North Atlantic region. The extension methodology is described in Section 2.4.

2.3 Methods

2.3.1 Statistical reconstruction (1748-1994)

Statistical reconstructions were developed separately for the two rainfall domains. For each domain and calendar month, two regression approaches were applied: Lasso and Random Forest (RF) regression. Models were developed independently for each calendar month to allow seasonally varying predictor-rainfall relationships and fitted using the 1930-1994 period, given the denser modern gauge network within the gridded observational dataset. Four-fold blocked cross-validation was used within the 1930-1994 period. Calibration years were ordered chronologically and divided into four contiguous blocks with out-of-fold predictions generated from temporally withheld data. These out-of-fold predictions were used to tune model

https://doi.org/10.5194/egusphere-2026-3352
Preprint. Discussion started: 7 July 2026
© Author(s) 2026. CC BY 4.0 License.

parameters, derive ensemble weights and to summarise model development performance. Selected LASSO and RF models were then refitted using the full 1930-1994 period and applied to the full record to generate monthly reconstructions for 1748-1994. Monthly predictions were subsequently aggregated to annual and seasonal totals. Seasons were defined as DJF, MAM, JJA, SON and MJJA, with December assigned to the following winter season-year for DJF aggregation. The 1930-1994 out-of-fold results are interpreted as blocked cross-validation model development diagnostics rather than as fully independent validation, because the same model development period was used for hyperparameter selection and ensemble weight derivation. Independent temporal validation was undertaken separately over 1865-1929, which was not used for model fitting, hyperparameter tuning or ensemble weighting. Model performance was summarised using root mean square error (RMSE), mean absolute error (MAE), Pearson's correlation coefficient, Spearman's rank correlation coefficient and percent bias (PBIAS).

2.3.1.1 Lasso Regression

Lasso (least absolute shrinkage and selection operator) regression is an extension of ordinary least squares (OLS) that remains stable when predictors are collinear and numerous (Tibshirani, 1996; Hastie et al., 2009). Stability is achieved by adding a penalty on coefficient size, which shrinks some estimates towards zero and sets others exactly to zero, thereby reducing overfitting relative to unpenalised OLS (Tetko et al., 1995; Li et al., 2020). Lasso regression was implemented in R using glmnet (Friedman et al., 2010). For each month, the penalty parameter (λ) was selected using four-fold blocked cross-validation over the 1930-1994 calibration period. Out-of-fold predictions from this procedure were retained to assess model skill within the calibration period. Final monthly Lasso models were then refitted using the full 1930-1994 calibration period and applied to the complete predictor record. Predictor importance was summarised using the absolute values of coefficients from the final model fitted to the whole 1930-1994 calibration period.

2.3.1.2 Random Forests

Random forests (RFs) are supervised machine learning methods that learn the relationship between predictors and a target variable from training data. RF regression builds an ensemble of regression trees by fitting each tree to a bootstrap resample of the training data and averaging predictions across trees (Breiman, 2001). Within each tree, splits are selected to reduce prediction error, typically by minimising the residual sum of squares. RF can represent

https://doi.org/10.5194/egusphere-2026-3352
Preprint. Discussion started: 7 July 2026
© Author(s) 2026. CC BY 4.0 License.

nonlinear responses and higher-order interactions, but is typically less interpretable than regression and can overfit in small samples without careful validation.

Random forest (RF) regression was implemented in R using randomForest (Liaw and Wiener, 2002). For each month, hyperparameters were tuned using the same four-fold blocked cross-validation scheme as for Lasso. A small grid search explored (i) mtry, the number of predictors randomly considered at each split, using three values based on p (the number of predictors) - the square root of p, p/4, and p/2 (rounded) and (ii) minimum node size (5, 10, 20, 30), with the number of trees fixed at 300. For each setting, cross-validated predictions were generated, and RMSE was computed. The configuration with the lowest cross-validated RMSE was selected, and the model was refitted to the whole 1930-1994 calibration period. Predictor importance was quantified using permutation importance, expressed as the percentage increase in out-of-bag (OOB) error after permuting each predictor.

2.3.1.3 Ensemble Generation

For each domain and calendar month, monthly rainfall reconstructions from both the Lasso and RF models were combined into a two-member weighted ensemble. Ensemble weights were derived from the blocked cross-validation out-of-fold RMSE values calculated over the 1930-1994 model-development period. These were converted to weights using an inverse-squared RMSE rule and normalised to sum to 1. The final monthly ensemble estimate was calculated as the weighted average of the final full-refit LASSO and RF predictions. Because weights were derived separately by month and domain, the relative contribution of LASSO and RF was allowed to vary seasonally and spatially between SA9 and SA-upland. Because the same model-development period was used both to tune the individual models and to derive ensemble weights, the out-of-fold ensemble performance is treated as a model-development diagnostic rather than as fully independent validation. Independent temporal validation was undertaken separately over 1865-1929, which was not used for model fitting, hyperparameter tuning or ensemble weighting.

2.3.1.4 Uncertainty Estimation for the Statistical Ensemble

Uncertainty in the statistical ensemble was estimated using non-parametric bootstrap resampling of the 1930-1994 calibration years. For each domain and calendar month, 1000 bootstrap samples were generated by sampling calibration years with replacement. For each bootstrap replicate, LASSO and RF models were refitted using the selected monthly model settings: the selected LASSO λ, selected RF mtry, selected RF node size and 300 trees. The

https://doi.org/10.5194/egusphere-2026-3352
Preprint. Discussion started: 7 July 2026
© Author(s) 2026. CC BY 4.0 License.

refitted models were then applied to the full predictor record, and the ensemble prediction was calculated using the previously derived month-specific inverse-RMSE² weights. Pointwise 95% uncertainty intervals were calculated as the 2.5th and 97.5th percentiles of the bootstrap ensemble of 1000 predictions. Monthly bootstrap predictions were aggregated to annual and seasonal totals to produce corresponding uncertainty intervals at those timescales. Any negative monthly rainfall predictions from the statistical models were truncated to zero before aggregation and the calculation of uncertainty intervals.

It should be noted that the derived intervals quantify uncertainty associated with calibration-sample resampling, conditional on the selected predictor set, gridded rainfall target, model structures, selected hyperparameters and ensemble-weighting scheme. They do not represent total reconstruction uncertainty. In particular, they do not fully account for uncertainty in predictor datasets, structural uncertainty associated with the choice of modelling framework, possible non-stationarity in predictor-rainfall relationships, or uncertainty in the gridded observational target itself. The intervals are therefore interpreted as conditional reconstruction intervals rather than comprehensive uncertainty bounds.

2.3.2 Jenkinson monthly reconstruction (1711-1977)

Monthly rainfall totals for each study domain were reconstructed from the Jenkinson anomaly-distribution dataset (Jenkinson et al., 1979) for 1711-1977 by anchoring its annual anomalies to a domain-specific mean annual rainfall (AAR) estimated over 1865-1975. Uncertainty in AAR was quantified using a non-parametric bootstrap of the annual totals for each domain from 1865 to 1975. A total of 1,000 resamples were generated by drawing years with replacement and calculating AAR for each resample. For each bootstrap AAR, Jenkinson annual percentage anomalies were converted to annual rainfall totals by scaling the AAR upward (for positive anomalies) or downward (for negative anomalies), thereby transferring the interannual variability encoded in Jenkinson onto the domain-specific climatological mean annual rainfall (AAR). Annual totals were then partitioned into monthly totals using the corresponding year's internal percentages (converted to proportions). Final monthly estimates were summarised across the 1,000-member ensemble using the median and the 2.5th and 97.5th percentiles as uncertainty intervals. These intervals reflect uncertainty in the anchored AAR estimate and are conditional on the Jenkinson anomalies and internal-percentage fields.

https://doi.org/10.5194/egusphere-2026-3352
Preprint. Discussion started: 7 July 2026
© Author(s) 2026. CC BY 4.0 License.

2.3.3 Oxygen-isotope reconstruction of MJJA rainfall (1200-2000)

Extended summer rainfall (May-August, MJJA) for each GDA domain was reconstructed from an annually resolved oak cellulose $\delta^{18}O$ master chronology for Central England using a reduced major axis variance-scaling approach as applied by Loader et al. (2020). For each domain, the calibration relationship was defined from the overlap period between $\delta^{18}O$ and observed MJJA rainfall over the period 1930-2000. Calibration-period means and standard deviations of $\delta^{18}O$ and MJJA rainfall, together with their correlation, were used to derive the transformation, which was then applied to all years with available $\delta^{18}O$ to generate a reconstructed MJJA rainfall series.

Uncertainty in reconstructed MJJA rainfall was quantified using 1000 bootstrap resamples of annual calibration-year pairs ($\delta^{18}O$, MJJA rainfall) drawn with replacement (Efron and Tibshirani, 1993). For each replicate, calibration summary statistics and the $\delta^{18}O$-rainfall correlation were re-estimated, and a complete reconstruction was generated using the ensemble median and the 2.5th and 97.5th percentiles as 95% uncertainty intervals. These intervals quantify uncertainty arising from calibration of the variance-scaling transformation and are conditional on the chosen target series and calibration window.

2.4 Extension of the Dublin Snow and Sleet series and residual-based analysis

To assess whether differences between the Jenkinson and statistical ensemble reconstructions may reflect snow- and sleet-related gauge undercatch in early observations, a residual-based diagnostic framework was adopted, following the rationale of Murphy et al. (2019). As this analysis requires a continuous estimate of precipitation phase variability over the reconstruction period, the Dublin Snow and Sleet (DSS) series was first extended back to 1748. To extend DSS prior to the earliest direct observations (1867), the long-term London snow and sleet series (1668-1974) compiled by Gordon Manley (1969) and digitised by Murphy et al. (2019) was used. A linear no-intercept transfer function between DSS and the Manley snow and sleet series was calibrated over their common period (1867-1974) using aggregated annual totals. The fitted relationship was then applied to the Manley series to estimate DSS values for 1748-1866, thereby rescaling the UK-based chronology to the Dublin domain. The resulting extended DSS series provides a temporally continuous indicator of snowfall and sleet occurrence for comparison with the rainfall reconstructions from the mid-eighteenth century onward and reproduces coherent interannual-to-decadal variability across the overlap period.

https://doi.org/10.5194/egusphere-2026-3352
Preprint. Discussion started: 7 July 2026
© Author(s) 2026. CC BY 4.0 License.

The extension of the DSS series was undertaken at an annual resolution. Residual analysis was subsequently performed using the difference series between the Jenkinson and ensemble rainfall reconstructions with annual Pearson's r, 10-year Pearson's r and significance of 10-year p-value following adjustment for autocorrelation calculated. This approach enables assessment of whether systematic differences between reconstructions covary with an independent indicator of snowfall and sleet variability, thereby providing an indication of potential snow-related undercatch in early rainfall observations used in the Jenkinson reconstruction.

Decadal analysis was undertaken to account for noise in the annual reconstructions, whereas beyond-10-year smoothing reduces the effective sample size for calculating nominal p-values. Comparison with residuals was undertaken for the DJF, MAM, and ONDJFMAM (snow year) periods, representing the seasons most sensitive to solid precipitation. Although separate seasonal DSS reconstructions were not developed, the annually resolved DSS series is dominated by cold-season snowfall variability and was therefore used as an independent indicator of years characterised by enhanced snow and sleet occurrence. To enable comparison across series, residuals and the extended DSS were standardised to z-scores using their respective means and standard deviations. For visual comparison, the DSS series was sign-inverted (multiplied by -1) so that periods of increased snow and sleet occurrence correspond to larger positive residuals.

2.5 Evaluation of reconstructions

Comparison of performances across the different reconstructions is undertaken using visual assessment and quantitative evaluation for the full period of overlap with observations. Key evaluation metrics include Pearson's r to assess covariation, R^2 to examine the proportion of variance in the observations captured by each reconstruction and the Percent Bias (PBIAS) and Mean Absolute Error (MAE). The sensitivity of winter and spring totals to undercatch of snow, particularly in the early observations, is evaluated by comparing reconstruction residuals with the extended Dublin Snow and Sleet (DSS) series (Section 2.4). Full reconstructions are presented and compared for concurrent periods.

The ability of each reconstruction to capture wet and dry extremes in the observations is evaluated using the Probability of Detection (POD) and False Alarm Ratio (FAR) (Murphy et al., 2020; Rudd et al., 2017). Based on threshold exceedances, the former measures the

https://doi.org/10.5194/egusphere-2026-3352
Preprint. Discussion started: 7 July 2026
© Author(s) 2026. CC BY 4.0 License.

proportion of observed extremes successfully detected by the reconstructions, while the latter measures the proportion of extremes in the reconstructions that were not observed. The metrics are calculated as follows:

$$POD = \frac{H}{H + M}$$

$$FAR = \frac{F}{H + F}$$

where hits (H) count the number of events which occurred in both the observations and the reconstruction, misses (M) indicate the number of events that occurred in the observed series but not in the reconstruction. The False Alarm (F) counts instances where an event occurred in the reconstruction but not in the observed series.

For continuous monthly reconstructions (Jenkinson and Statistical Ensemble), the Standardised Precipitation Index (SPI) was derived for both reconstructions and observations. SPI was fitted for accumulation periods of 1, 3, 6 and 12 months using a Gamma distribution. POD and FAR were evaluated at thresholds of +/- 1.0 and +/-1.5, representing moderate and extreme droughts and pluvials. For MJJA precipitation, per cent anomalies relative to a fixed (1980-2000) baseline, were calculated for each series. Positive and negative thresholds of +/- 20% and +/- 50% of the baseline for each month were identified.

We assess the consistency of the top 20 wettest and driest years between 1865 and 1977 across each reconstruction and observations using the Jaccard Similarity Coefficient (Jaccard Index, JI). For our subset of the top 20 wet and dry years, the JI is used to measure the similarity/diversity of sample sets and is calculated as:

$$JI(A, B) = \frac{|A \cap B|}{|A \cup B|}$$

Where the numerator represents the intersection of the two sets or the number of events in common, and the denominator represents the total number of unique events present across both lists. A JI score of 1 indicates identical sets, 0 indicates complete disjoint (no overlap) while a value of ~0.33 indicates 50% overlap.

In addition to quantitative evaluation against observations, reconstructed rainfall variability was assessed qualitatively using long-term UK precipitation series (Section 2.2.5). Seasonal totals (DJF, MAM, JJA, SON) were standardised (z-scores) separately for each station and

https://doi.org/10.5194/egusphere-2026-3352
Preprint. Discussion started: 7 July 2026
© Author(s) 2026. CC BY 4.0 License.

season using the mean and standard deviation over 1711-1977 and then smoothed using 10-year forward running means. These series provide an independent regional benchmark for examining the timing, persistence, and relative magnitude of wet and dry periods in the Dublin pre-instrumental period. Comparisons are based on visual assessment of temporal alignment and consistency across series.

3 Results

3.1 Calibration and Evaluation

3.1.1 Statistical Reconstructions

Statistical reconstructions demonstrate clear skill in reproducing rainfall variability in both domains during the calibration (1930-1994) period. For ease of presentation, cross-validation results for each domain and model are provided in the Supplement (Tables S1-S2), with only ensemble results for final models presented below. For both domains, Lasso regression marginally outperforms Random Forests in each month and for seasonal and annual aggregations and contributes slightly greater weight to the final ensemble.

Table 2 reports results for the weighted ensemble mean performance over the full calibration period (1930-1994) and an independent evaluation period (1865-1929), while Figure 2 shows scatter plots of ensemble reconstructions by domain for each season and annually. For SA9 the weighted ensemble mean returns calibration period r values >0.85 for all months, with PBIAS typically < 5 per cent. For the independent evaluation period, skill typically reduces slightly, with some months (April, July, October, and November) showing r values between 0.60 and 0.70. The largest PBIAS scores are evident for June (12.32%) and September (16.55%). For other months, PBIAS is well below 10%. On a seasonal and annual basis, the ensemble reconstructions for SA9 typically show good performance and transferability between periods, with best performance in winter and the largest decrease in performance in autumn (SON), where r falls from 0.84 to 0.63. However, the PBIAS for all seasons and annual totals remains within 5% for both calibration and validation periods. Similar performance characteristics are evident for SA-upland, but PBIAS scores are slightly higher. Here the largest dis-improvement in skill, moving from calibration (r = 0.92) to validation (0.76), is for extended summer (MJJA). It is difficult to confirm whether decreases in performance moving from calibration to validation are due to data inhomogeneities in the early record or to overfitting. The strong

https://doi.org/10.5194/egusphere-2026-3352
Preprint. Discussion started: 7 July 2026
© Author(s) 2026. CC BY 4.0 License.

performance of the models and the ensemble for cross-validation during the calibration window would suggest that data inhomogeneities cannot be ruled out.

There are notable differences in the predominant predictors used in each model between SA9 and SA-upland. For the majority of months in both domains, sea level pressure is the dominant predictor, most often LSLP, followed by g50. For SA9 in the winter months, the next most important predictor is the Paris-London index (pl), a surrogate for the NAO. However, in the SA-upland this is typically replaced by the EU index, whereas in spring and summer the pl index remains more important than in the lowland SA9.

https://doi.org/10.5194/egusphere-2026-3352
Preprint. Discussion started: 7 July 2026
© Author(s) 2026. CC BY 4.0 License.

Season	Period	SA9 - Ensemble				SA-upland - Ensemble			
		RMSE	Pearson's R	MAE	PBIAS	RMSE	Pearson's R	MAE	PBIAS
Jan	1930-1994	15.41	0.90	11.72	0.08	26.37	0.89	20.36	0.07
	1865-1929	20.23	0.78	16.58	3.88	39.18	0.70	30.45	5.80
Feb	1930-1994	14.31	0.91	11.20	0.00	19.70	0.92	15.42	0.06
	1865-1929	18.11	0.81	14.41	-0.77	30.75	0.80	23.64	0.67
Mar	1930-1994	16.10	0.86	12.99	-0.04	26.13	0.85	21.44	-0.13
	1865-1929	19.38	0.74	14.75	0.32	35.30	0.69	27.20	5.74
Apr	1930-1994	10.36	0.91	7.73	0.18	17.99	0.88	14.02	-0.10
	1865-1929	19.19	0.68	14.75	4.25	30.09	0.66	24.21	4.99
May	1930-1994	18.73	0.85	13.98	0.16	22.94	0.90	16.65	0.12
	1865-1929	20.98	0.74	17.50	8.54	27.17	0.78	22.11	13.60
Jun	1930-1994	16.50	0.88	12.53	0.07	18.55	0.90	14.64	0.13
	1865-1929	21.83	0.76	18.35	12.32	27.44	0.76	23.49	8.25
Jul	1930-1994	15.15	0.89	12.16	0.10	14.68	0.94	11.41	0.14
	1865-1929	27.27	0.65	20.49	-3.80	32.89	0.70	27.26	4.51
Aug	1930-1994	17.01	0.88	14.04	0.10	21.25	0.92	16.94	0.10
	1865-1929	28.88	0.71	22.19	-6.27	33.16	0.73	26.33	0.33
Sep	1930-1994	18.04	0.89	14.76	-0.14	22.63	0.91	18.56	-0.20
	1865-1929	25.32	0.77	21.86	16.55	40.17	0.71	33.34	18.34
Oct	1930-1994	20.89	0.86	16.01	-0.16	28.61	0.86	21.58	-0.16
	1865-1929	28.86	0.67	21.26	-0.84	42.89	0.66	31.84	-6.44
Nov	1930-1994	20.42	0.84	15.58	-0.09	30.80	0.84	23.71	0.24
	1865-1929	24.89	0.67	19.07	-1.73	34.36	0.71	27.45	6.10
Dec	1930-1994	17.87	0.87	13.92	0.01	26.39	0.89	21.62	-0.09
	1865-1929	26.48	0.84	22.21	9.32	46.44	0.81	38.58	12.53
Annual	1930-1994	62.96	0.83	50.57	0.01	94.90	0.84	76.01	0.01
	1865-1929	86.49	0.71	67.02	2.97	148.94	0.71	119.06	5.76
DJF	1930-1994	30.53	0.89	23.69	-0.16	44.24	0.92	36.23	-0.20
	1865-1929	36.03	0.86	28.91	4.76	69.21	0.79	56.25	6.98
MAM	1930-1994	27.33	0.86	19.81	0.10	40.72	0.89	30.40	-0.04
	1865-1929	31.70	0.75	25.36	4.30	53.80	0.71	42.73	7.91
JJA	1930-1994	29.70	0.88	22.79	0.09	33.45	0.91	25.22	0.12
	1865-1929	42.35	0.75	31.78	-0.60	53.71	0.79	40.91	3.78
SON	1930-1994	36.07	0.84	28.69	-0.13	53.95	0.83	42.47	-0.04
	1865-1929	47.99	0.63	38.45	3.71	69.23	0.61	56.11	4.68
MJJA	1930-1994	33.90	0.89	26.59	0.11	38.57	0.92	30.39	0.12
	1865-1929	47.48	0.69	38.05	1.35	62.33	0.76	49.40	5.94

Table 2 Performance of monthly, annual and seasonal rainfall reconstructions for the weighted ensemble over the calibration (1930-1994) and independent validation (1865-1929) periods in the SA9 and SA-upland domains. Model skill is quantified using root mean square error (RMSE), mean absolute error (MAE), Pearson's correlation coefficient (R) and percent bias (PBIAS). Ensemble estimates are derived from a weighted combination of the Lasso and RF models based on inverse-squared RMSE. Seasons are defined as DJF (winter), MAM (spring), JJA (summer), SON (autumn), and MJJA (May-August).

https://doi.org/10.5194/egusphere-2026-3352
Preprint. Discussion started: 7 July 2026
© Author(s) 2026. CC BY 4.0 License.

527

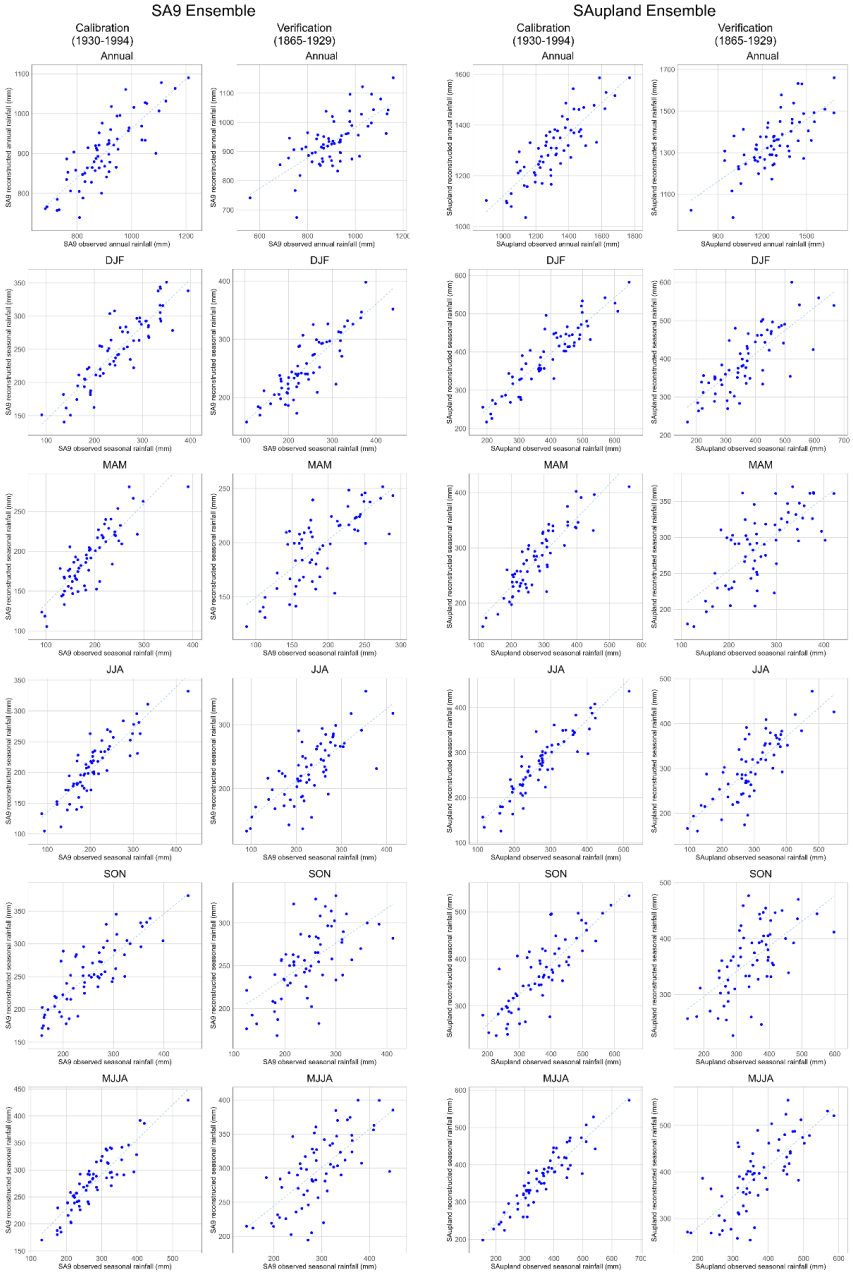

528

529 **Figure 2 Observed versus reconstructed rainfall for the weighted ensemble mean (weighted mean of**
530 **LASSO and Random Forest) at annual and seasonal timescales (DJF, MAM, JJA, SON, and MJJA) in the**
531 **SA9 (left) and SA-upland (right). Calibration results for 1930-1994 are shown in the left columns, and**
532 **independent validation results for 1865-1929 in the right columns.**

https://doi.org/10.5194/egusphere-2026-3352
Preprint. Discussion started: 7 July 2026
© Author(s) 2026. CC BY 4.0 License.

3.1.2 Jenkinson Reconstructions

The Jenkinson reconstruction is evaluated over the full overlap with observations (1865-1977). While this series lacks independence from the observations, it remains important to quantify its performance relative to the modern best estimate of rainfall across domains. The bootstrap distribution of annual average rainfall is shown in Figure 3, indicating the higher totals in the SA-upland and greater variability in the AAR samples. Median reconstructions show clear skill at monthly and seasonal scales, with generally strong correlations and a large proportion of the variability explained, indicating that they reproduce the broad structure of SA9 rainfall variability (Table 3). Skill is strongest in winter (DJF) and summer (JJA), while SON is the weakest season in both domains. At the monthly scale, correlations are high throughout most of the year. In SA9 r ranges from 0.82 in October to 0.94 in June, while in SA-upland r ranges from 0.83 in October to 0.91 in May and June. PBIAS is greatest in January in SA9 (11.29%) and in June in SA_updand (7.76%). Figure 4 provides scatter plots between observed seasonal totals and Jenkinson reconstructions. The reconstructions' performance is evident, with some increased error at higher totals in MAM and MJJA in both domains.

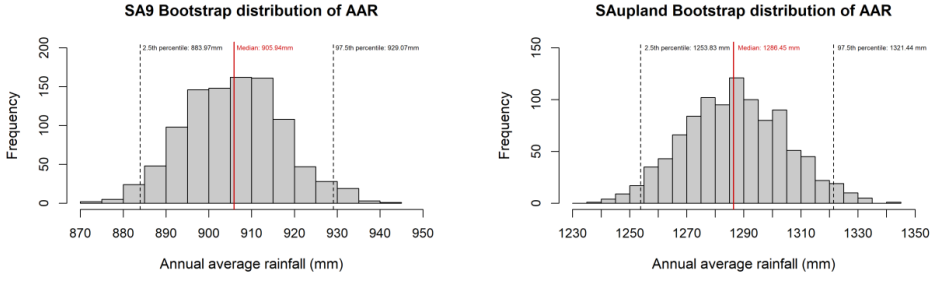

Figure 3 Bootstrap distribution of the SA9 (left) and SA-upland (right) annual average rainfall (AAR), based on 1000 resamples of annual totals for the period 1865-1977, obtained by resampling with replacement from the observed annual totals.

https://doi.org/10.5194/egusphere-2026-3352
Preprint. Discussion started: 7 July 2026
© Author(s) 2026. CC BY 4.0 License.

	SA9				SA-upland			
Period	**RMSE**	**Pearson's R**	**MAE**	**PBIAS**	**RMSE**	**Pearson's R**	**MAE**	**PBIAS**
Jan	17.83	0.90	14.38	11.29	30.50	0.84	24.51	0.97
Feb	13.58	0.92	10.59	5.4	25.27	0.87	19.26	-3.39
Mar	14.3	0.88	10.41	0.83	26.26	0.86	19.02	-7.46
Apr	10.89	0.90	8.26	-3.93	18.31	0.88	14.06	-3.35
May	14.53	0.90	10.72	-7.01	18.08	0.91	14.21	-0.30
Jun	11.76	0.94	8.31	-4.28	17.09	0.92	14.03	7.76
Jul	16.08	0.90	12.30	-5.05	22.50	0.87	16.95	4.70
Aug	18.4	0.90	12.61	-5.47	23.55	0.88	18.67	5.23
Sept	15.82	0.91	12.10	1.4	26.93	0.87	20.83	5.53
Oct	23.02	0.82	16.82	2.72	35.20	0.78	26.35	1.50
Nov	17.62	0.88	13.69	5.59	25.77	0.88	19.70	1.84
Dec	18.08	0.91	14.14	8.23	33.16	0.87	22.96	0.78
Annual	60.05	0.87	47.77	1.29	102.54	0.85	82.47	1.14
DJF	34.12	0.91	28.80	8.53	53.54	0.86	41.47	-0.12
MAM	23.85	0.87	17.96	-3.36	39.30	0.85	29.76	-3.89
JJA	30.19	0.91	22.52	-5.00	40.24	0.90	30.83	5.73
SON	35.19	0.84	29.22	3.29	55.55	0.80	45.16	2.80
MJJA	34.51	0.9	26.18	-5.45	44.17	0.89	34.25	4.34

Table 3 Skill metrics for the SA9 and SA-upland Jenkinson rainfall reconstructions at monthly, annual and seasonal timescales, including MJJA (May-August). Model performance is evaluated using root mean square error (RMSE), Pearson's correlation coefficient (R), mean absolute error (MAE) and percent bias (PBIAS), computed from matched observed and reconstructed totals over the full period of overlap between observed and reconstructed series (1865-1977).

https://doi.org/10.5194/egusphere-2026-3352
Preprint. Discussion started: 7 July 2026
© Author(s) 2026. CC BY 4.0 License.

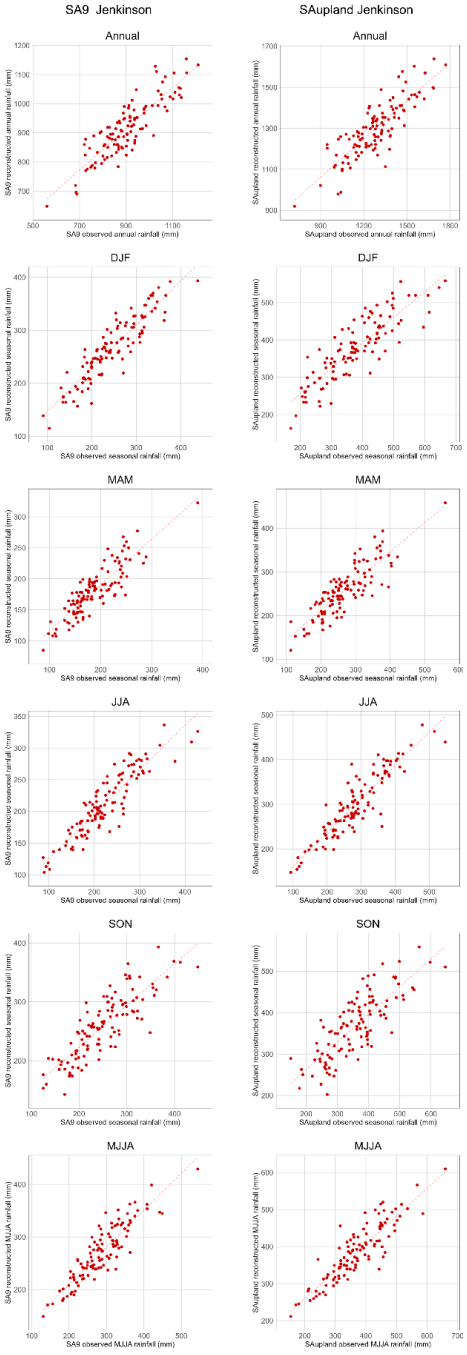

564

565 **Figure 4 Observed versus reconstructed SA9 (left) and SA-upland (right) rainfall for the Jenkinson-based**
566 **reconstructions over 1865-1977 at annual and seasonal timescales (DJF, MAM, JJA, SON, and MJJA).**

https://doi.org/10.5194/egusphere-2026-3352
Preprint. Discussion started: 7 July 2026
© Author(s) 2026. CC BY 4.0 License.

3.1.3 $\delta^{18}O$ Reconstructions

The $\delta^{18}O$-based reconstruction provides an independent estimate of MJJA rainfall variability, calibrated over 1930-2000 and evaluated against observations for 1865-1929 (Table 4; Figure 5). The reconstructed series shows a moderate and consistent relationship with observed MJJA rainfall in both domains across both calibration (SA9: r = 0.56; SA-upland: r = 0.54) and validation (SA9: r = 0.52; SA-upland: r = 0.54) periods. PBIAS scores are also very small for both domains. Split-period calibrations using early and late subsets of the overlap period (Table S3) yield comparable performance, indicating that the proxy-rainfall relationship is not strongly sensitive to the choice of calibration window.

Period	SA9		SA-upland	
	Calibration 1930-2000	Validation 1865-1929	Calibration 1930-2000	Validation 1865-1929
RMSE	66.57	68.54	90.48	90.44
Pearson	0.56	0.52	0.54	0.54
MAE	51.87	55.49	73.51	75.86
PBIAS	>-0.01	-1.15	>-0.01	2.45

Table 4 Performance metrics for the $\delta^{18}O$-based MJJA (May-August) rainfall reconstruction in the SA9 and SA-upland domains. Model performance is reported for the calibration period (1930-2000) and an independent validation period (1865-1929). Metrics include root mean square error (RMSE), mean absolute error (MAE), Pearson's correlation coefficient (r), and percent bias (PBIAS), calculated from matched observed and reconstructed seasonal totals. Reconstructed values correspond to the median of the bootstrap ensemble.

https://doi.org/10.5194/egusphere-2026-3352
Preprint. Discussion started: 7 July 2026
© Author(s) 2026. CC BY 4.0 License.

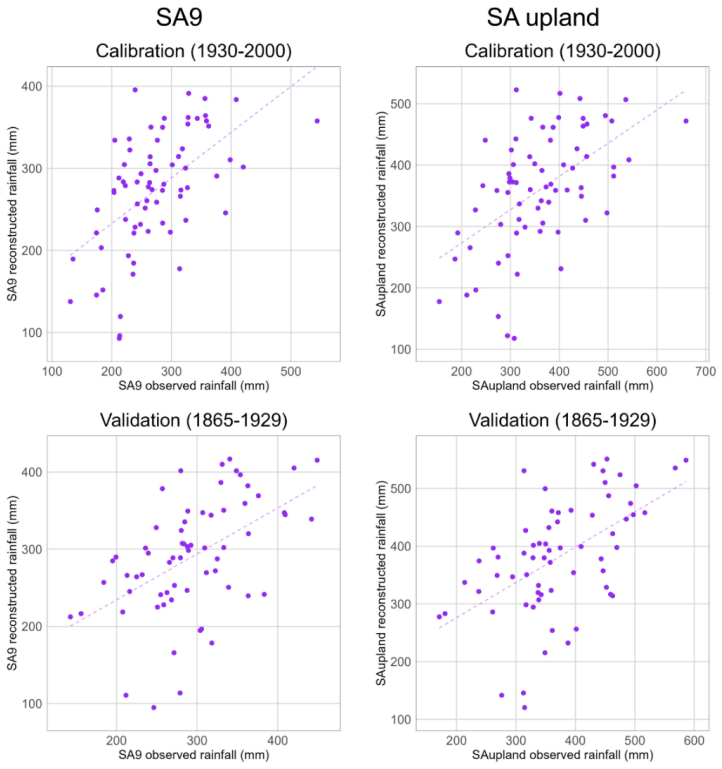

Figure 5 Observed versus reconstructed MJJA rainfall totals for SA9 (left) and SA upland (right) based on the tree-ring $\delta^{18}O$ reconstruction. Panels show calibration (1930-2000; top) and validation (1865-1929; bottom) periods. Reconstructed values represent the median model estimates for each year. Each point corresponds to an individual year, and dashed lines indicate least-squares linear regression fits, illustrating model performance during calibration and independent validation.

3.2 Performance over a common period

Given that each method required different calibration approaches, we next compare the performance of each reconstruction across the common overlap with observations 1865-1977, and visualise annual and seasonal reconstructions for their respective periods of record. Both the weighted ensemble and Jenkinson reconstructions reproduce observed rainfall variability in SA9 and SA-upland well at annual, seasonal and monthly scales. However, as expected, the Jenkinson reconstruction generally shows the stronger agreement with observations (Table 5). At the annual scale (Table 5 and Figure 6), both reconstructions capture broad interannual rainfall variability in each domain. The Jenkinson reconstruction is more closely aligned with the observed record, with higher correlations and lower errors than the ensemble in both

https://doi.org/10.5194/egusphere-2026-3352
Preprint. Discussion started: 7 July 2026
© Author(s) 2026. CC BY 4.0 License.

	SA9							
	Ensemble				Jenkinson			
Period	RMSE	MAE	Pearson's R	PBIAS	RMSE	MAE	Pearson's R	PBIAS
Jan	18.75	14.93	0.84	1.94	17.83	14.38	0.9	11.29
Feb	16.41	12.84	0.86	0.37	13.58	10.59	0.92	5.4
Mar	18.52	14.41	0.79	0.85	14.3	10.41	0.88	0.83
Apr	15.78	11.53	0.77	3.07	10.89	8.26	0.9	-3.93
May	20	15.98	0.77	4.1	14.53	10.72	0.9	-7.01
Jun	19.64	16.02	0.81	8.1	11.76	8.31	0.94	-4.28
Jul	23.06	17.01	0.74	-3.85	16.08	12.3	0.9	-5.05
Aug	24.31	18.45	0.79	-3.13	18.4	12.61	0.9	-5.47
Sep	22.73	19	0.81	6.65	15.82	12.1	0.91	1.4
Oct	26.06	19.41	0.76	-1.08	23.02	16.82	0.82	2.72
Nov	23.82	18.23	0.75	-1.52	17.62	13.69	0.88	5.59
Dec	23.09	18.49	0.83	6.05	18.08	14.14	0.91	8.23
Annual	78.62	61.69	0.76	1.61	60.05	47.77	0.87	1.29
DJF	34.13	26.97	0.86	3.01	34.12	28.8	0.91	8.53
MAM	29.9	22.93	0.78	2.67	23.85	17.96	0.87	-3.36
JJA	37.56	27.95	0.81	-0.31	30.19	22.52	0.91	-5
SON	43.42	34.4	0.74	1.14	35.19	29.22	0.84	3.29
MJJA	41.8	32.8	0.79	0.68	34.51	26.18	0.9	-5.45
	SA-upland							
	Ensemble				Jenkinson			
Period	RMSE	MAE	Pearson's R	PBIAS	RMSE	MAE	Pearson's R	PBIAS
Jan	34.89	26.62	0.79	2.52	30.5	24.51	0.84	0.97
Feb	26.43	19.95	0.86	1.17	25.27	19.26	0.87	-3.39
Mar	32.47	25.53	0.76	4.14	26.26	19.02	0.86	-7.46
Apr	25.56	19.87	0.75	4.14	18.31	14.06	0.88	-3.35
May	24.85	19.82	0.82	7.25	18.08	14.21	0.91	-0.3
Jun	24.09	19.76	0.82	5.76	17.09	14.03	0.92	7.76
Jul	27.02	20.91	0.8	1.67	22.5	16.95	0.87	4.7
Aug	27.83	21.44	0.82	1.12	23.55	18.67	0.88	5.23
Sep	33.91	27.19	0.79	8.35	26.93	20.83	0.87	5.53
Oct	37.65	27.68	0.75	-4.6	35.2	26.35	0.78	1.5
Nov	34.04	27.01	0.78	3.14	25.77	19.7	0.88	1.84
Dec	39.16	31.54	0.82	7.18	33.16	22.96	0.87	0.78
Annual	130.64	103.42	0.75	3.3	102.54	82.47	0.85	1.14
DJF	60.5	48.54	0.83	3.97	53.54	41.47	0.86	-0.12
MAM	48	37.18	0.77	5.13	39.3	29.76	0.85	-3.89
JJA	45.96	34.32	0.84	2.56	40.24	30.83	0.9	5.73
SON	63.39	50.3	0.73	1.92	55.55	45.16	0.8	2.8
MJJA	52.62	40.9	0.83	3.65	44.17	34.25	0.89	4.34

Table 5 Performance metrics for the weighted ensemble and Jenkinson reconstructions relative to observed rainfall in SA9 and SA-upland over the common period 1865-1977, evaluated at monthly, seasonal and annual scales. Metrics include root mean square error (RMSE), mean absolute error (MAE), Pearson's correlation coefficient (r), and percent bias (PBIAS).

https://doi.org/10.5194/egusphere-2026-3352
Preprint. Discussion started: 7 July 2026
© Author(s) 2026. CC BY 4.0 License.

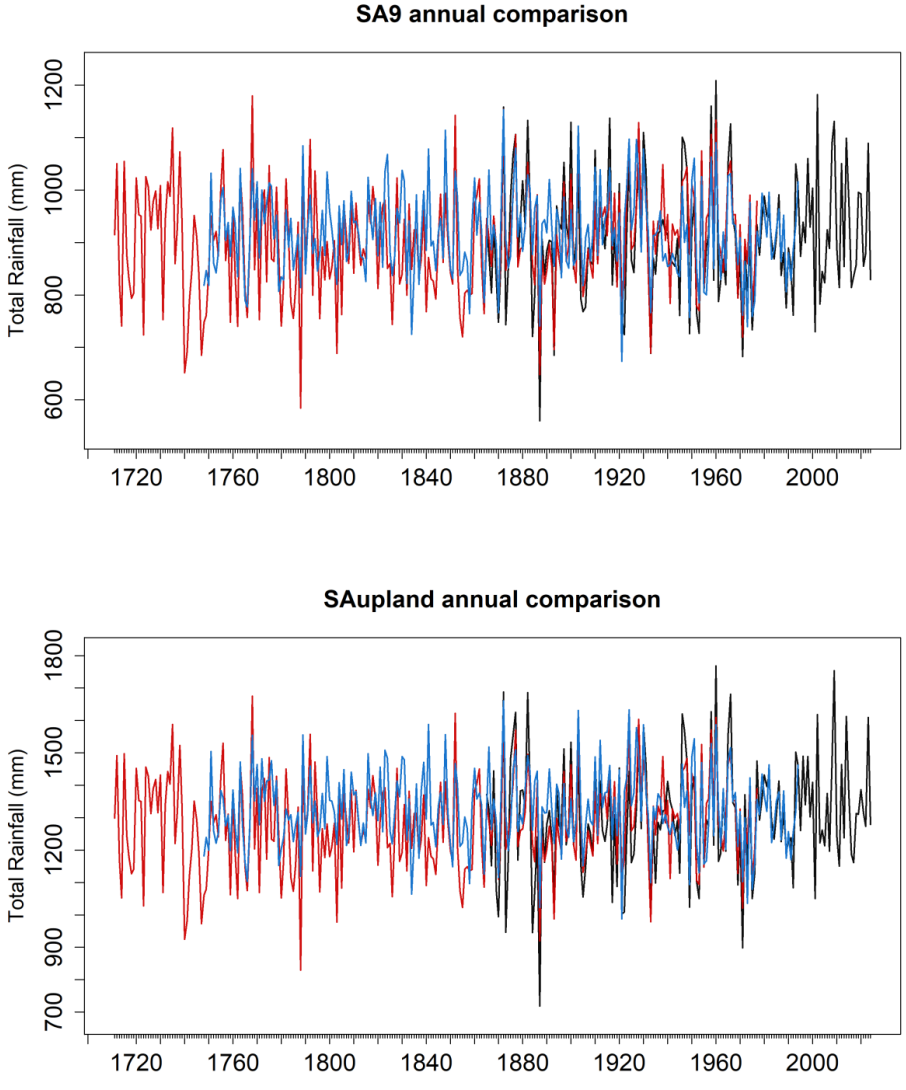

606

607 **Figure 6 Comparison of annual SA9 and SA-upland rainfall totals from the statistical and Jenkinson**
608 **reconstructions and the observations. The blue line represents the weighted ensemble reconstruction (1748-**
609 **1994), while the red line shows the Jenkinson-based reconstruction (1711-1977). The black line shows the**
610 **observed rainfall (1865-2024). All values are expressed as annual totals (mm).**

https://doi.org/10.5194/egusphere-2026-3352
Preprint. Discussion started: 7 July 2026
© Author(s) 2026. CC BY 4.0 License.

SA9 and SA-upland. In SA9, annual rainfall correlation is 0.87 for the Jenkinson reconstruction compared with 0.76 for the weighted ensemble, while RMSE falls from 78.62 mm for the ensemble to 60.05 mm for Jenkinson. A similar pattern is found in SA-upland, where annual correlation rises from 0.75 for the weighted ensemble to 0.85 for Jenkinson, accompanied by a reduction in RMSE from 130.64 mm to 102.54 mm. Biases are small for both methods, indicating that the main differences lie in their ability to capture year-to-year variability rather than mean totals.

At the seasonal scale (Table 5 and Figure 7), the Jenkinson reconstruction again outperforms the weighted ensemble across nearly all seasons and in both domains. In SA9, the highest seasonal performance is obtained for winter and summer. For DJF, correlations are 0.91 for Jenkinson and 0.86 for the ensemble, while in JJA the contrast is larger, with correlations of 0.91 and 0.81, respectively. MAM and SON show the same ordering, with Jenkinson correlations of 0.87 and 0.84, compared with 0.78 and 0.74 for the ensemble. Errors are also consistently lower for Jenkinson, especially in spring, summer and autumn. The same broad pattern is evident in SA-upland. Correlations for the weighted ensemble range from 0.73 in SON to 0.84 in JJA, whereas Jenkinson correlations range from 0.80 in SON to 0.90 in JJA. Thus, although both reconstructions reproduce observed seasonality, the Jenkinson approach provides a closer representation of seasonal rainfall variability in both domains, given the integration of observed data.

https://doi.org/10.5194/egusphere-2026-3352
Preprint. Discussion started: 7 July 2026
© Author(s) 2026. CC BY 4.0 License.

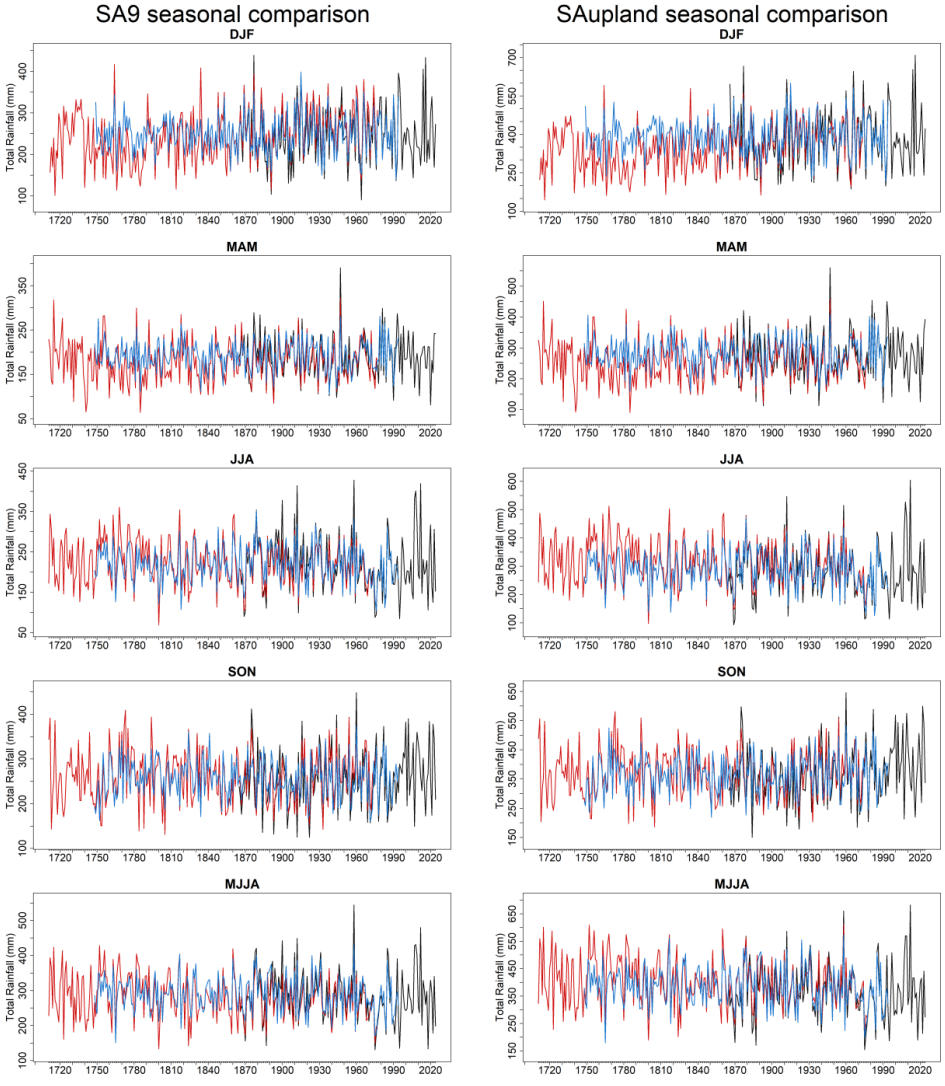

631

632 **Figure 7 Comparison of seasonal SA9 (left) and SA-upland (right) rainfall totals from the statistical and**
633 **Jenkinson reconstructions and observations. Panel shows DJF, MAM, JJA, SON, and MJJA totals. The**
634 **blue line represents the weighted ensemble mean reconstruction (1748-1994), while the red line shows the**
635 **Jenkinson-based reconstruction (1711-1977). The black line shows observed rainfall (1865-2024). All values**
636 **are expressed as seasonal totals (mm).**

637

638

639

https://doi.org/10.5194/egusphere-2026-3352
Preprint. Discussion started: 7 July 2026
© Author(s) 2026. CC BY 4.0 License.

The monthly results (Table 5) show a similar, and in some respects even clearer, contrast between the two approaches. For SA9, the weighted ensemble monthly correlations range from 0.74 in July to 0.86 in February, while Jenkinson ranges from 0.82 in October to 0.94 in June. In the SA-upland, ensemble correlations range from 0.75 in April and October to 0.86 in February, while Jenkinson ranges from 0.78 in October to 0.92 in June. Thus, monthly skill is consistently high for both reconstructions, but almost always higher for Jenkinson.

The MJJA season is particularly important because it permits comparison among all three reconstruction approaches (Table 6 and Figure 8). In SA9, the Jenkinson reconstruction shows the strongest agreement with observations, with r = 0.90, RMSE = 34.51 mm and MAE = 26.18 mm. The weighted ensemble performs less well, with r = 0.79, RMSE = 41.80 mm and MAE = 32.80 mm. The $\delta^{18}O$ reconstruction is markedly weaker, with a correlation of 0.54 and substantially larger errors (RMSE = 67.97 mm; MAE = 54.25 mm). In the SA-upland, the same ranking is observed: Jenkinson again performs best (r = 0.89; RMSE = 44.17 mm), followed by the weighted ensemble (r = 0.83; RMSE = 52.62 mm), while the $\delta^{18}O$ reconstruction remains much weaker (r = 0.54; RMSE = 90.91 mm). Notably, all three approaches show relatively small PBIAS values.

Overall, the verification results show that both primary monthly reconstructions provide credible representations of historical rainfall variability. However, the Jenkinson reconstruction performs best relative to observations across nearly all temporal aggregations and in both spatial domains. This is not surprising given the use of early observations in the Jenkinson series. For MJJA, the $\delta^{18}O$-based reconstruction provides a longer independent perspective, but its agreement with observed rainfall during 1865-1977 is notably weaker than that of either of the other two approaches.

	Ensemble				Jenkinson				$\delta^{18}O$ reconstruction			
Domain	**RMSE**	**MAE**	**Pearson's R**	**PBIAS**	**RMSE**	**MAE**	**Pearson's R**	**PBIAS**	**RMSE**	**MAE**	**Pearson's R**	**PBIAS**
SA9	41.80	32.80	0.79	0.68	34.51	26.18	0.90	-5.45	67.97	54.25	0.54	-0.21
SA-upland	52.62	40.9	0.83	3.65	44.17	34.25	0.89	4.34	90.91	75.01	0.54	1.96

Table 6 Performance metrics for the weighted ensemble mean, Jenkinson, and $\delta^{18}O$-based reconstructions relative to observed MJJA (May-August) rainfall in SA9 and SA-upland over the common period 1865-1977. Metrics include root mean square error (RMSE), mean absolute error (MAE), Pearson's correlation coefficient (r) and percent bias (PBIAS).

https://doi.org/10.5194/egusphere-2026-3352
Preprint. Discussion started: 7 July 2026
© Author(s) 2026. CC BY 4.0 License.

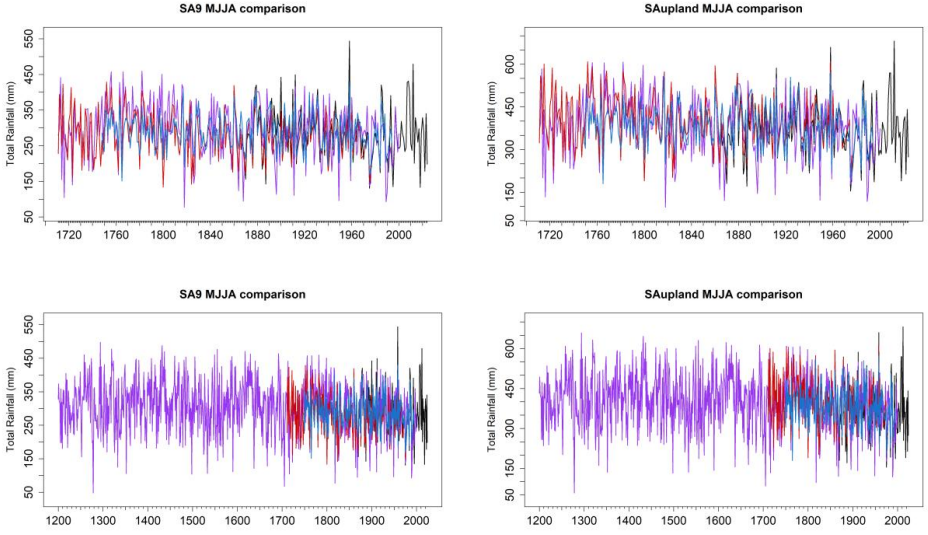

669

670 **Figure 8 Comparison of MJJA (May-August) SA9 (left) and SA-upland (right) rainfall totals from all three**
671 **reconstruction approaches. The blue line represents the weighted ensemble reconstruction (1748-1994), the**
672 **red line shows the Jenkinson-based reconstruction (1711-1977), and the purple line denotes the tree-ring**
673 **$\delta^{18}O$-based reconstruction (1711-2000 on the top and 1200-2000 on the bottom). Black segments indicate**
674 **observed rainfall used to extend the reconstructions beyond their respective reconstruction periods (1978-**
675 **2024 for the Jenkinson series, 1995-2024 for the ensemble, and 2001-2024 for the $\delta^{18}O$-based**
676 **reconstruction). All values are expressed as seasonal totals (mm).**

https://doi.org/10.5194/egusphere-2026-3352
Preprint. Discussion started: 7 July 2026
© Author(s) 2026. CC BY 4.0 License.

3.3 Representation of extremes 1865-1977

The ability of the Jenkinson and weighted ensemble to capture wet and dry extremes is evaluated for the common period of overlap across the reconstructions using SPI-based threshold exceedances (Figure 9). Across all accumulation periods and thresholds, the Jenkinson reconstruction demonstrates the highest skill at identifying both wet and dry events, with a higher Probability of Detection (POD) and lower False Alarm Ratio (FAR) than the statistical models. This is evident for both moderate (±1.0) and more extreme (±1.5) thresholds, where Jenkinson retains comparatively high detection rates, particularly for dry events, which are generally detected more reliably than wet events across all reconstructions. Jenkinson reconstructions also achieve comparatively lower false alarm ratios, with POD values of 0.72 (wet) and 0.76 (dry) for Jenkinson compared to 0.56 and 0.67 for the ensemble for SPI-3, and correspondingly lower FAR values (0.32 and 0.26 vs 0.43 and 0.39), with similar differences evident across SPI-1, SPI-6 and SPI-12 (Figure 9).

The statistical reconstructions exhibit lower skill and greater variability. Random Forest performs more favourably than LASSO, particularly for dry events, where POD values approach those of the Jenkinson reconstruction at longer accumulation periods. However, this is often accompanied by elevated FAR (Figure 9). The weighted ensemble mean typically performs between the two methods, improving on Lasso but not fully matching the performance of Random Forest or Jenkinson. Differences between methods are most apparent at shorter accumulation periods (SPI-1 and SPI-3).

For the more extreme thresholds (±1.5), detection skill decreases across all reconstructions, reflecting the increased difficulty in identifying rarer events. However, the relative ranking of model performance remains consistent, with Jenkinson retaining the highest POD and generally lower FAR. In contrast, the statistical models show reduced POD and increased false alarm rates, particularly for wet extremes. Dry extremes are generally better captured than wet extremes across all methods (Figure 9).

https://doi.org/10.5194/egusphere-2026-3352
Preprint. Discussion started: 7 July 2026
© Author(s) 2026. CC BY 4.0 License.

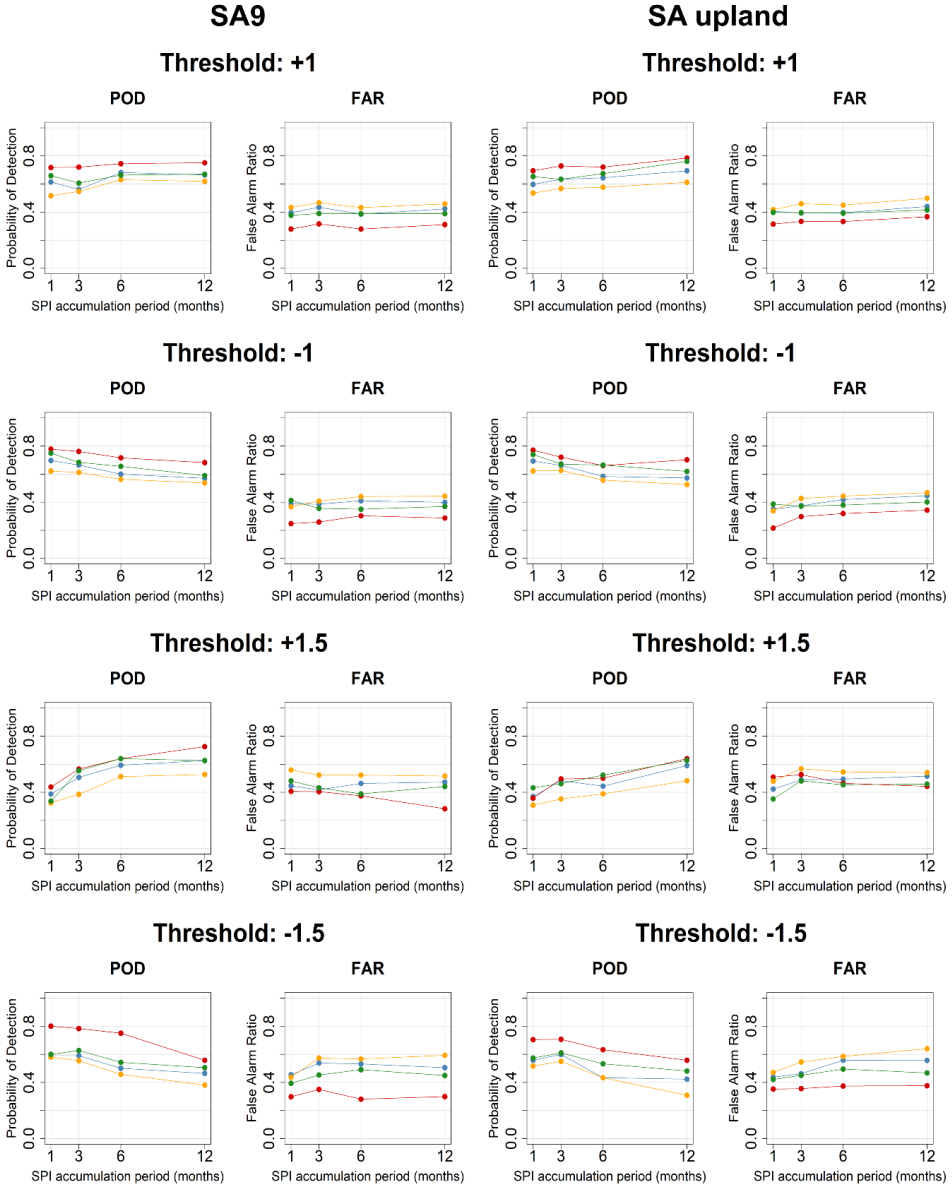

Figure 9 Skill of the reconstruction methods in detecting wet and dry events, evaluated using the Probability of Detection (POD), False Alarm Ratio (FAR) for SA9 (left) and SA upland (right). Results are shown for four threshold levels (±1 and ±1.5) and across SPI accumulation periods (1, 3, 6, and 12 months). Each panel displays the performance of the Jenkinson (red), Lasso (orange), Random Forest (green), and the ensemble (blue) reconstruction. Positive thresholds (+1, +1.5) represent wet extremes, while negative thresholds (-1, -1.5) represent dry extremes. Higher POD values indicate better skill, whereas lower FAR values indicate fewer false detections.

https://doi.org/10.5194/egusphere-2026-3352
Preprint. Discussion started: 7 July 2026
© Author(s) 2026. CC BY 4.0 License.

The Jaccard Index is employed to evaluate the skill of all three reconstructions in capturing the top 20 wettest and driest years and seasons (Figure 10), with the full lists of top 20 wettest and driest years provided in Table S4. The Jenkinson reconstruction shows the highest agreement with observations in identifying the top 20 wettest and driest years across most seasons and at the annual scale, with JI values generally exceeding those of the weighted ensemble. For example, in SA9, the Jenkinson reconstruction captures 16 of the 20 wettest (JI = 0.67) and 14 of the 20 driest (JI = 0.54) years, compared to 13 (JI = 0.48) and 10 (JI = 0.33) years, respectively, for the ensemble. This pattern is consistent across seasons in both SA9 and SA-upland (Tables S5-S6), with the Jenkinson reconstruction typically identifying a larger proportion of extreme years than the weighted ensemble. The wettest years (1865-1977) in the observed series for both domains are 1960 and 1872 (ranked third in SA9 and second in SA-upland). Both reconstructions identify these years as exceptionally wet, with 1872 ranked as the wettest, and 1960 ranked second in the Jenkinson reconstruction in both domains, and fifth (SA9) and fourth (SA-upland) in the ensemble (Table S4). The driest years in the observed record are 1887 and 1971. The Jenkinson reconstruction identifies 1887 as the driest year in both domains, while 1971 is ranks fourth. The weighted ensemble reconstruction also identifies these years as exceptionally dry, ranking 1887 as the third- and second-driest year in the SA9 and SA-upland domains, respectively, and 1971 as the sixth- and seventh-driest year (Table S4).

In winter (DJF), both reconstructions perform well, capturing 13-15 events (JI = 0.48-0.60), while in spring (MAM) and summer (JJA) the advantage of the Jenkinson reconstruction is more pronounced, identifying 14-15 events (JI = 0.48-0.60) compared to 10-12 events (JI = 0.33-0.43) for the weighted ensemble. In autumn (SON)' wet extremes show the weakest agreement, with Jenkinson and the ensemble identifying 11 and 10 of the top 20 events, respectively (JI = 0.38 and 0.33). In contrast, dry extremes are captured more reliably, with 16 and 14 events identified (JI = 0.67 and 0.54, respectively).

Across both domains, dry extremes are generally captured more reliably than wet extremes, with higher Jaccard Index values and a greater number of correctly identified events across most seasons. This is particularly evident in autumn (SON), where dry extremes show the highest agreement (JI up to 0.67), while wet extremes exhibit the lowest agreement (JI typically 0.33-0.38). For MJJA, inclusion of the $\delta^{18}O$ reconstruction highlights its more limited ability to reproduce extreme years, capturing 9-11 of the top 20 events (JI = 0.29-0.38), compared to 12 events (JI = 0.43) for the weighted ensemble and 15-16 events (JI = 0.60-0.67) for the

https://doi.org/10.5194/egusphere-2026-3352
Preprint. Discussion started: 7 July 2026
© Author(s) 2026. CC BY 4.0 License.

Jenkinson reconstruction. JI values for the $\delta^{18}O$ reconstruction are substantially lower than those of both Jenkinson and the ensemble, particularly for dry extremes, indicating reduced skill in identifying individual extreme years. Notably, for SA9, the $\delta^{18}O$ reconstruction captures just under 50 per cent of the observed driest years in MJJA, and just over 50 per cent of the wettest years. This behaviour is reversed for SA-upland, while the weighted ensemble shows improved performance in the upland domain, particularly for dry extremes where agreement matches that of the Jenkinson reconstruction.

https://doi.org/10.5194/egusphere-2026-3352
Preprint. Discussion started: 7 July 2026
© Author(s) 2026. CC BY 4.0 License.

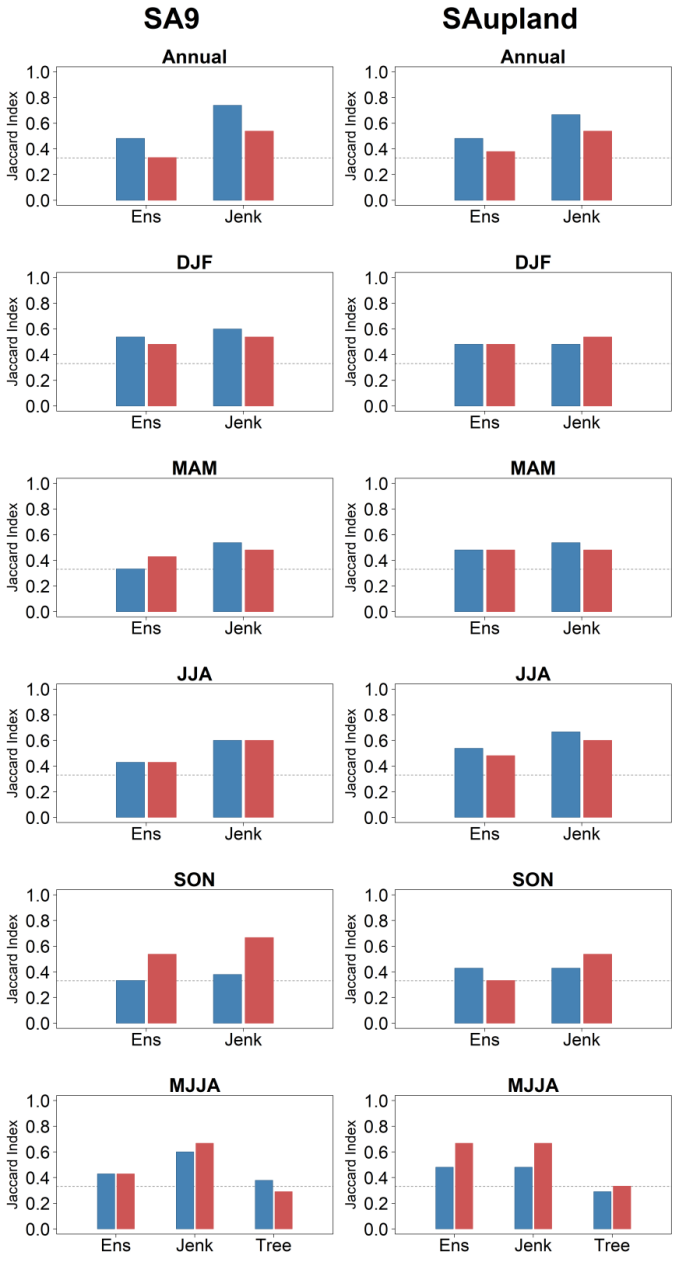

Figure 10 Agreement between reconstructed and observed extreme precipitation years, expressed using the Jaccard Index (JI) for SA9 (left) and SA-upland (right) across six seasonal aggregations (Annual, DJF, MAM, JJA, SON, MJJA). Bars represent the agreement in the identification of the top wettest (blue) and driest (red) years between model reconstructions and observations. Higher JI values indicate stronger agreement between reconstructed and observed extreme years, while the dashed horizontal line indicates a JI value of 0.33, corresponding approximately to a 50% overlap.

https://doi.org/10.5194/egusphere-2026-3352
Preprint. Discussion started: 7 July 2026
© Author(s) 2026. CC BY 4.0 License.

3.4 Full period reconstructions

Comparisons thus far have focused on the period of overlap with observations; in this section we focus primarily on the pre-1865 reconstructions. For winter (DJF), while both Jenkinson and the weighted ensemble show good coherence over the instrumental period, there is evidence of divergence between reconstructions in both domains before circa 1850, with DJF totals for Jenkinson generally lower than for the ensemble (Figure 7). The divergence is more apparent in the upland domain. A similar pattern is also evident in spring (MAM), but less marked. Given that the Jenkinson series is constructed directly from early observations and documentary sources (Dr John Rutty's weather diary), we explore whether these reconstructions are sensitive to observational bias through the under-representation of snow due to changes in gauge design, observational practice or reliance on documentary sources (Murphy et al., 2020). The weighted ensemble reconstruction is less likely to contain such biases, as it is derived from predictors such as sea level pressure, among others, rather than direct precipitation observations.

To explore whether snowfall and sleet variability may contribute to divergence between reconstructions, a residual series was calculated as the difference between the Jenkinson and weighted ensemble mean and compared with an annually resolved extended Dublin Snow and Sleet (DSS) series derived using the Manley London snow and sleet chronology. A linear transfer function (slope of 0.55 (95% CI 0.51-0.60) calibrated over the common period (1867-1974) showed good agreement between the Dublin and Manley series ($r = 0.83$; MAE = 4.8 days and Percent Bias of -6.48%), supporting the use of the extended DSS chronology prior to the instrumental overlap period. The derived extended DSS series is shown in Figure S1. Comparison of 10-year forward-running averages for reconstruction residuals and the inverted DSS series is presented in Table 10 and Figure 11 for winter (DJF), spring (MAM), and the snow year (ONDJFMAM). Both DJF and the snow year show significant ($p < 0.05$) positive correlations with the residual series at the annual scale, with the snow year 10-year smoothed series also revealing significance after p-value correction for autocorrelation in SA9. No significant correlation is found for MAM, whereas for DJF, 10-year smoothing reduces significance once p-values are corrected ($p < 0.10$). Visual correspondence between the residual and DSS series is evident across all seasons and both domains, with periods of elevated snow and sleet occurrence generally coinciding with larger divergence between the reconstruction approaches. Similar behaviour across both domains is consistent with the possibility that the pre-1865 Jenkinson winter and spring series may exhibit low biases due to snowfall undercatch,

https://doi.org/10.5194/egusphere-2026-3352
Preprint. Discussion started: 7 July 2026
© Author(s) 2026. CC BY 4.0 License.

795 changing observational practices, or limitations in documentary and early instrumental sources.
796 Comparison with reconstructions and available long-term series from the UK is broadly
797 consistent with the interpretation that winter totals in the 18th-century Jenkinson series may be
798 biased low relative to the weighted ensemble (Figure 12), while also lending support to the
799 large-scale hydroclimatic variability captured by the weighted ensemble mean. Comparison
800 with Pauling et al. (2006) reconstructions for SA9 winter (DJF) totals reinforces the finding
801 that the Jenkinson reconstruction underestimates winter totals, with the Pauling reconstructions
802 showing stronger agreement with the weighted ensemble reconstruction. The winter Jenkinson
803 reconstruction for SA9 reveals a correlation of 0.68 with the Pauling reconstruction, while the
804 equivalent correlation for the weighted ensemble is 0.73 (Figure 13).

805

		r		p-value		adjusted p-value	
season	**smoothing**	**SA9**	**SA_Upland**	**SA9**	**SA_Upland**	**SA9**	**SA_Upland**
DJF	annual	0.46	0.47	0.00	0.00	0.00	0.00
DJF	10-year	0.72	0.70	0.00	0.00	0.09	0.09
MAM	annual	0.08	0.08	0.41	0.41	0.42	0.42
MAM	10-year	0.32	0.29	0.00	0.00	0.46	0.51
ONDJFMAM	annual	0.42	0.41	0.00	0.00	0.00	0.00
ONDJFMAM	10-year	0.73	0.66	0.00	0.00	0.04	0.08

806

807 **Table 10 Pearson's correlations between annual and smoothed (10-year forward running mean) residuals**
808 **and the inverse extended snow and sleet residuals for each domain. Also shown are the raw and adjusted**
809 **p-values when the effective sample size is reduced due to autocorrelation from smoothing.**

810

811 For Spring (MAM) good coherence is evident between reconstructions and longer-term
812 reconstructions with the Jenkinson series showing lower decadal totals than the weighted
813 ensemble during the 1700s, but consistent with some UK stations (Figure 12). Comparison of
814 the annual MAM series with Pauling et al. (2006) reconstructions shows strong agreement with
815 the weighted ensemble mean, with Jenkinson revealing lower annual totals prior to 1780
816 (Figure 13).

https://doi.org/10.5194/egusphere-2026-3352
Preprint. Discussion started: 7 July 2026
© Author(s) 2026. CC BY 4.0 License.

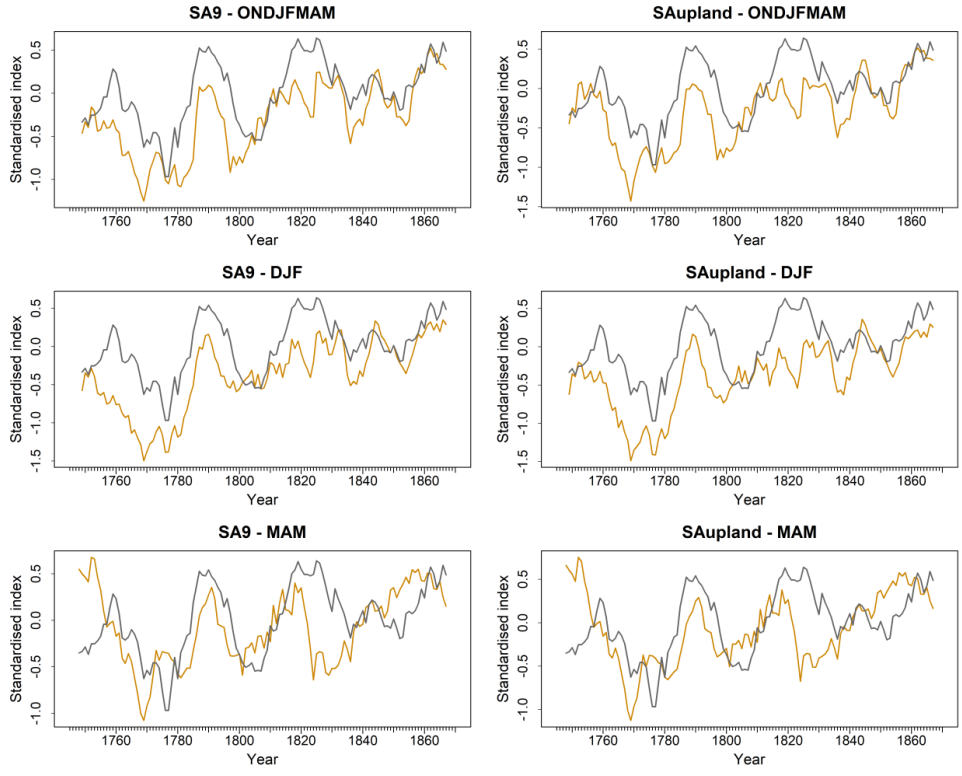

Figure 11 Standardised residuals (Jenkinson minus weighted ensemble; black) and inverted extended Dublin Snow and Sleet (DSS) series (orange) for the SA9 and SA-upland domains across ONDJFMAM, DJF, and MAM aggregations, 1748-1867. Series are expressed as z-scores and smoothed using 10-year forward running means. The annually resolved extended DSS series was sign-inverted to facilitate visual comparison, such that periods of enhanced snow and sleet occurrence correspond to larger positive residuals.

In summer (JJA), both the Jenkinson and the weighted ensemble reconstructions show close agreement back to circa 1810. For earlier years, the Jenkinson series shows higher seasonal totals than the ensemble, especially in the upland domain. For extended summer (MJJA), better agreement is evident, but the Jenkinson series shows elevated totals relative to the ensemble for certain years in the latter half of the 18th-century. For autumn (SON), there is good agreement between the two approaches throughout the full reconstructions period.

Comparison of summer reconstructions with UK stations reveals that some UK stations (Spalding and Kew) show similarly high totals in the second half of the 1700s. Other stations (Oxford and Carlisle) tend to show closer correspondence to the weighted ensemble reconstructions in this period (Figure 12). Comparison with Pauling et al. (2006)

https://doi.org/10.5194/egusphere-2026-3352
Preprint. Discussion started: 7 July 2026
© Author(s) 2026. CC BY 4.0 License.

reconstructions for SA9 adds weight to the view that summer totals in this period are too high in the Jenkinson reconstruction (Figure 13). For MJJA the $\delta^{18}O$ reconstruction tends to agree with the Jenkinson series during this period. However, divergence between the $\delta^{18}O$ reconstruction and other observed and reconstructed series is evident in the early and late 1700s. The period 1730-1800 is subject to uncertainty about the extent and magnitude of wet summers. As the Jenkinson reconstruction during this period is strongly informed by Rutty's Dublin weather diary (1716-1765) and sparse early instrumental observations, it remains difficult to determine whether the elevated summer totals reflect genuine hydroclimatic conditions or uncertainties associated with documentary and early observational sources. This period is marked by notable spatial gradients in summer totals, which would be worth unpacking in future research. Autumn shows strong agreement across all reconstructions and available series throughout the record (Figure 12).

https://doi.org/10.5194/egusphere-2026-3352
Preprint. Discussion started: 7 July 2026
© Author(s) 2026. CC BY 4.0 License.

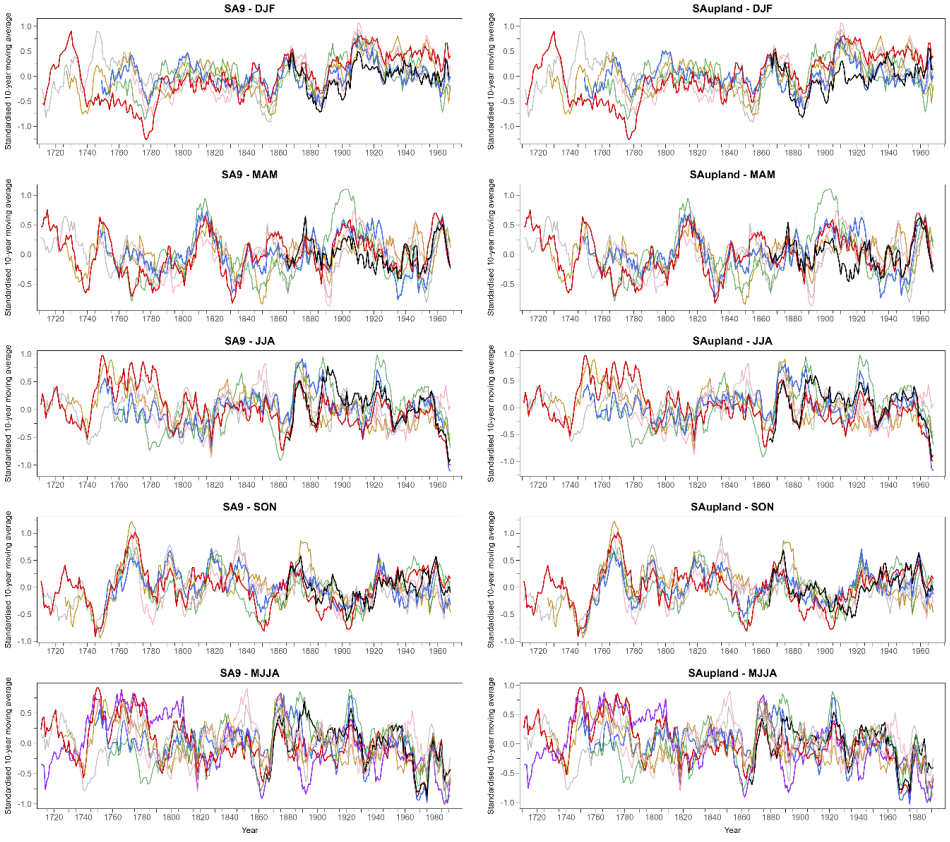

Figure 12 Seasonal and MJJA standardised 10-year moving averages for the SA9 (left) and SA-upland (right) domains, compared with instrumental series from selected UK stations. Panels show winter (DJF), spring (MAM), summer (JJA), autumn (SON), and May-August (MJJA). Coloured lines represent individual station series (Kew - grey, Spalding - orange, Carlisle - green, Oxford - pink), weighted ensemble (blue) and Jenkinson-based reconstructions (red). The black line denotes the observed series, and the purple line in the MJJA panels represents the $\delta^{18}O$ reconstruction. All series are standardised to a common baseline to facilitate comparison of variability across datasets. Note that the MJJA series extends over a longer period (1711-2000) than the seasonal panels (1711-1977).

https://doi.org/10.5194/egusphere-2026-3352
Preprint. Discussion started: 7 July 2026
© Author(s) 2026. CC BY 4.0 License.

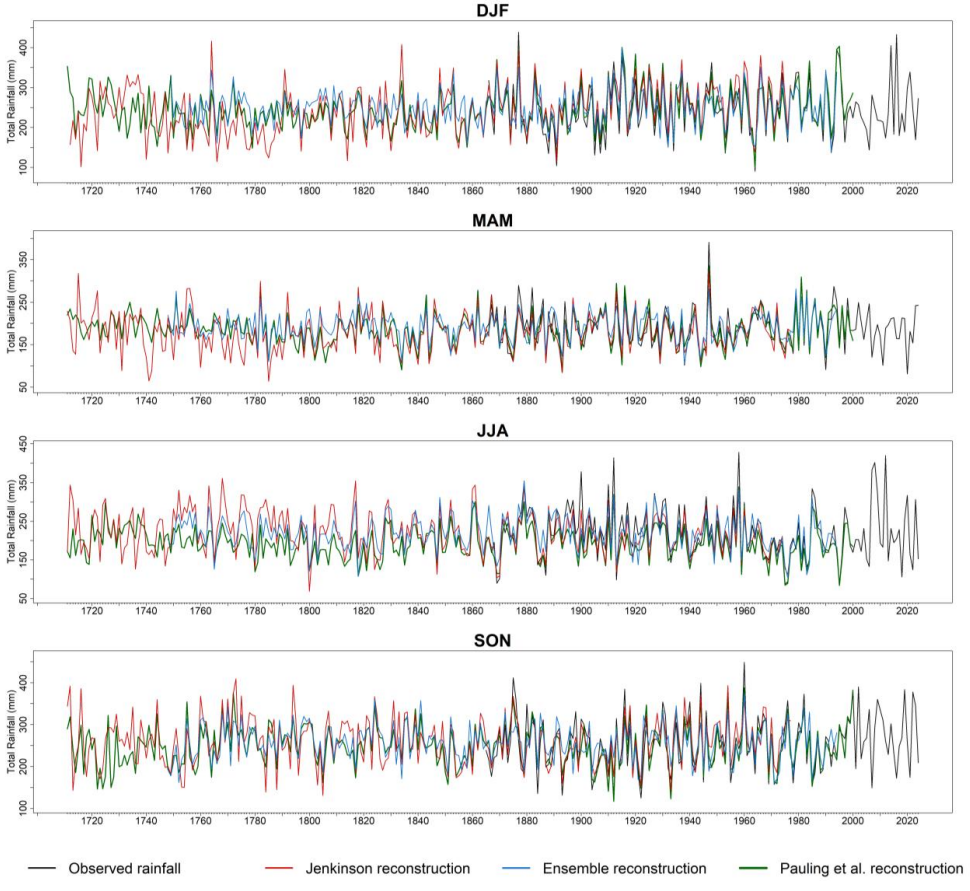

Figure 13 Comparison of seasonal totals for SA9 from observations, Pauling et al. (2006) reconstructions, the weighted ensemble mean and the Jenkinson reconstruction from 1711 to 2024.

4 Discussion

This study developed and evaluated multi-method precipitation reconstructions for two water resource zones in the Greater Dublin Area (GDA) in Ireland, with direct relevance to water resource planning. All three reconstruction approaches show robust skill in reproducing rainfall variability across contrasting lowland and upland domains and provide complementary perspectives on GDA hydroclimate, extending rainfall variability into the early eighteenth century while placing recent summer conditions within a longer-term context extending to 1200 CE. This reflects the growing recognition that hydroclimatic reconstruction is strengthened by integrating documentary, instrumental, circulation-based, and proxy evidence

https://doi.org/10.5194/egusphere-2026-3352
Preprint. Discussion started: 7 July 2026
© Author(s) 2026. CC BY 4.0 License.

rather than relying on a single method (Pauling et al., 2006; Murphy et al., 2018; Brázdil et al., 2018; Brönnimann et al., 2019a, 2019b).

Across the common observational overlap period (1865-1977), the Jenkinson reconstruction shows the strongest agreement with observations at annual, seasonal, monthly, and event-based scales, likely reflecting the direct incorporation of early instrumental evidence. The statistical ensemble also performs well but exhibits smoother variability and compressed extremes, consistent with the variance reduction observed in regression-based reconstruction approaches (Bürger, 2007; Hastie et al., 2009). In contrast, the $\delta^{18}O$ reconstruction shows weaker interannual agreement with observations, as expected, given that tree-ring isotope signals integrate broader growing-season hydroclimatic conditions rather than discrete precipitation events and are focused on central England (McCarroll and Loader, 2004; Gessler et al., 2014; Klesse et al., 2018).

Importantly, we show that strong reconstruction performance during the nineteenth- and twentieth-century overlap period does not necessarily imply equal reliability earlier in the record. This is particularly relevant for the Jenkinson reconstruction, as the underlying source composition changes substantially over time. During the later overlap period, the reconstruction benefits from improved instrumental coverage and more standardised observational practices, whereas earlier sections, particularly prior to the mid-nineteenth century, rely more heavily on documentary evidence and sparse rain-gauge observations. Divergence between the Jenkinson and weighted ensemble reconstructions is most evident in winter and spring prior to the mid-nineteenth century, particularly in the upland domain. Residual analysis shows broad correspondence between reconstruction divergence and the extended Dublin Snow and Sleet (DSS) series, suggesting that snowfall and mixed-precipitation undercatch may contribute to low biases in the early Jenkinson winter and spring series. This hypothesis is also supported through comparison with available seasonal reconstructions by Pauling et al. (2006). Similar observational biases associated with historical precipitation measurement have been linked to rain-gauge exposure, snowfall measurement, and early observational practices (Strangeways, 1996; Strangeways, 2010; Pollock et al., 2018), while comparable inhomogeneities have also been identified in long-term Irish and UK precipitation records (Murphy et al., 2018; Murphy et al., 2019).

In contrast, although the statistical ensemble generally exhibits lower validation skill during the instrumental overlap, its use of independent predictors is less vulnerable to changes in input

https://doi.org/10.5194/egusphere-2026-3352
Preprint. Discussion started: 7 July 2026
© Author(s) 2026. CC BY 4.0 License.

confidence over time. However, this approach assumes that the relationship between circulation-based predictors and Dublin-domain rainfall calibrated during 1930-1994 remains sufficiently stable back to 1748. These results highlight that reconstruction approaches possess differing uncertainty structures and temporal sensitivities that must be considered when interpreting long-term hydroclimatic variability. Comparison with long-term UK rainfall series and Pauling et al. (2006) reconstructions further supports this interpretation, with several records aligning more closely with the weighted ensemble reconstruction during eighteenth-century winters. Consequently, while the Jenkinson reconstruction likely provides the strongest event-scale representation during the later eighteenth and nineteenth centuries (given its incorporation of observed data), the ensemble reconstruction may offer a more robust estimate of earlier winter and spring hydroclimatic variability where snowfall-related biases are likely greatest.

The mid-eighteenth century emerges as a particularly uncertain period for reconstructing summer rainfall. Although the Jenkinson and ensemble reconstructions show broad coherence during much of the observational period, substantial divergence is evident during the latter half of the eighteenth century, particularly for JJA and MJJA rainfall in the upland domain. Comparison with independent UK rainfall series, Pauling et al. (2006) reconstructions, and the $\delta^{18}O$ reconstruction does not provide a single coherent interpretation of this period. While stations such as Spalding and Kew show elevated summer totals comparable to the Jenkinson reconstruction, Oxford and Carlisle align more closely with the ensemble reconstruction. The $\delta^{18}O$ chronology also shows partial agreement with the Jenkinson series during this interval, although disagreement remains substantial. Rather than representing model error, this divergence may reflect genuine spatial hydroclimatic heterogeneity across Britain and Ireland, with strong regional gradients in summer rainfall variability during the eighteenth century. Similar heterogeneous behaviour has been identified in European precipitation reconstructions (Pauling et al., 2006; Casty et al., 2007; Cook et al., 2015; Brázdil et al., 2020b). Consequently, the period 1730-1800 should be regarded as an important uncertainty window for reconstructed summer rainfall variability requiring further investigation across multiple data sources.

The $\delta^{18}O$ reconstruction provides an important longer-term perspective on hydroclimatic variability that is unavailable from documentary and instrumental sources alone. The chronology is most valuable as an indicator of low-frequency summer hydroclimatic variability rather than as an event-scale reconstruction. Although agreement with observations is weaker at interannual timescales, the reconstruction nevertheless retains meaningful hydroclimatic

https://doi.org/10.5194/egusphere-2026-3352
Preprint. Discussion started: 7 July 2026
© Author(s) 2026. CC BY 4.0 License.

skill. This likely reflects both the integrated nature of tree-ring isotope signals and the spatial mismatch between Central England oak cellulose and Dublin hydroclimate.

While a significant advance for understanding rainfall variability for a major European city, future work should focus on improved uncertainty propagation, incorporation of additional Irish documentary and proxy evidence, spatially resolved reconstructions, and hydrological evaluation of reconstructed droughts and water-resource vulnerability (e.g. Brázdil et al., 2018; Peña-Angulo et al., 2022; Jobbová et al., 2024). Some additional limitations should also be acknowledged. The Jenkinson reconstruction and observational series are unlikely to be fully independent during the overlap period, with some station data contributing to both datasets.

Taken together, the reconstructions are best interpreted as complementary products with different strengths and applications. The Jenkinson reconstruction is most suitable for later-period monthly and seasonal variability and event-scale analysis, where validation against observations is strongest. The statistical ensemble provides an independent circulation-informed reconstruction that offers a physically interpretable representation of monthly regional hydroclimatic variability and provides a more robust basis for interpreting early winter and spring conditions where snowfall-related observational biases are greatest. Our work also shows that despite calibration to a sparser observational dataset, the Pauling et al. (2006) reconstructions remain a robust estimate of seasonal totals in the lowland SA9 region, extending back to the early 1700s. In contrast, the $\delta^{18}O$ chronology is most useful for placing MJJA rainfall variability within a longer-term hydroclimatic context rather than identifying individual extreme years.

Beyond methodological evaluation, these reconstructions also provide an extended hydroclimatic baseline relevant to drought risk assessment and long-term water resource planning in eastern Ireland. The reconstructions provide the basis for placing recent droughts within a longer-term hydroclimatic context and for identifying periods and extremes that are not fully represented within the short instrumental record. Such information may support hydrological modelling, stress-testing of water-resource systems, and assessment of historical droughts. The differing strengths of the reconstruction approaches are also important operationally, as confidence in reconstructed hydroclimatic variability depends on season, period, and intended application.

https://doi.org/10.5194/egusphere-2026-3352
Preprint. Discussion started: 7 July 2026
© Author(s) 2026. CC BY 4.0 License.

5 Conclusion

This study presents a multi-method reconstruction of precipitation variability for the Greater Dublin Area, integrating documentary, instrumental, circulation-based indices, and tree-ring isotope evidence. Independent monthly reconstructions were developed for lowland and upland water-resource domains using the Jenkinson rainfall dataset and a statistical ensemble based on Lasso and Random Forest models, while an oak cellulose $\delta^{18}O$ chronology was used to extend May-August rainfall back to 1200 CE. Across the observational overlap period, both the Jenkinson reconstruction and the statistical ensemble reproduce broad rainfall variability, but the Jenkinson reconstruction shows the strongest agreement with observations at monthly, seasonal, annual, and event scales, given that this series integrates the earliest observations in Ireland. The statistical ensemble provides a physically interpretable, circulation-based reconstruction, although it tends to smooth variability and under-represent extremes. The $\delta^{18}O$ reconstruction shows weaker interannual agreement with observed MJJA rainfall but provides an independent perspective on longer-term summer hydroclimatic variability.

Reconstruction performance over the instrumental overlap does not imply uniform reliability through time. Prior to the mid-nineteenth century, winter and spring divergence between the Jenkinson and weighted ensemble mean reconstructions is consistent with possible snow- and sleet-related undercatch in early precipitation sources. Summer rainfall during the eighteenth century is also uncertain, with differences among the Dublin reconstructions, the $\delta^{18}O$ chronology, and the long-term UK rainfall series and other seasonal reconstructions suggesting genuine regional hydroclimatic heterogeneity. Used together, these reconstructions provide a stronger basis for contextualising droughts, pluvials, and seasonal rainfall variability affecting the Greater Dublin Area. For water-resource and climate-risk applications, the reconstructions extend the range of hydroclimatic variability available for stress-testing beyond the instrumental period and hydrological evaluation of reconstructed drought and pluvial episodes.

https://doi.org/10.5194/egusphere-2026-3352
Preprint. Discussion started: 7 July 2026
© Author(s) 2026. CC BY 4.0 License.

Author contribution:

Conceptualization and methodology, CM, CH; Formal analysis, CH; Resources, CR, CM; Data curation, CH, CR; Statistical analysis and visualisation, CH; Writing - original draft preparation, CH; Writing - review and editing, CH, CM, CR; Supervision, CM, CR; All authors contributed to interpretation of the findings and approved the final manuscript.

Competing interests:

The authors declare that they have no conflict of interest.

Data and code availability:

The datasets and code supporting this study are openly available through the Zenodo repository at https://doi.org/10.5281/zenodo.20605305.

The repository contains the input datasets used for the statistical, documentary and tree-ring rainfall reconstructions, R scripts required to reproduce the reconstruction workflows, calibration and uncertainty estimation procedures, and the derived reconstruction products for both the SA9 and SA-upland study domains. These include the monthly rainfall reconstructions, associated 95% uncertainty intervals, extended snow and sleet (SS) series, tree-ring reconstructions, and accompanying documentation describing the repository structure and individual workflows. README files are provided to describe the required input data, folder structure, and execution workflow, thereby facilitating reproduction of the analyses.

Acknowledgements:

The authors gratefully acknowledge Met Éireann for providing the gridded precipitation dataset that formed an integral component of this study.

Financial support:

This research was funded by the Irish Research Council (IRC) through the IRC Government of Ireland Postgraduate Scholarship Programme (IRC/GOIPG/2022/1844).

https://doi.org/10.5194/egusphere-2026-3352
Preprint. Discussion started: 7 July 2026
© Author(s) 2026. CC BY 4.0 License.

References

Adam, J. C., and Lettenmaier, D.P.: Adjustment of global gridded precipitation for systematic bias, Journal of Geophysical Research: Atmospheres, 108(D9), 4257, 10.1029/2002JD002499, 2003.

Barnston, A.G., and Livezey, R.E.: Classification, Seasonality and Persistence of Low-Frequency Atmospheric Circulation Patterns, Monthly Weather Review, 115(6), pp.1083-1126, https://doi.org/10.1175/1520-0493(1987)115<1083:CSAPOL>2.0.CO;2, 1987.

Blöschl, G., Kiss, A., Viglione, A. et al. : Current European flood-rich period exceptional compared with past 500 years, Nature, 583(7817), pp.560-566, https://doi.org/10.1038/s41586-020-2478-3, 2020.

Brázdil, R., Dobrovolný, P., Bauch, M., Camenisch, C., Kiss, A., Kotyza, O., Oliński,P. and Řezníčková: Central Europe, 1531-1540 CE: The driest summer decade of the past five centuries?, Climate of the Past, 16(6), pp.2125-2151, https://doi.org/10.5194/cp-16-2125-2020, 2020a.

Brázdil, R., Kiss, A., Luterbacher, J., Nash, D. J., and Řezníčková, L.: Documentary data and the study of past droughts: a global state of the art, Climate of the Past, 14(12), pp.1915-1960, https://doi.org/10.5194/cp-14-1915-2018, 2018.

Brázdil, R., Kiss, A., Řezníčková, L., Barriendos, M.: Droughts in Historical Times in Europe, as Derived from Documentary Evidence, In: Herget, J., Fontana, A. (eds) Palaeohydrology - Traces, Tracks and Trails of Extreme Events, Springer, Cham, pp.65-96, https://doi.org/10.1007/978-3-030-23315-0_4, 2020b.

Breiman, L.: Random Forests, Machine Learning, 45(1), pp.5-32, https://doi.org/10.1023/A:1010933404324, 2001.

Brönnimann, S., Allan, R., Ashcroft, L. et al.: Unlocking Pre-1850 Instrumental Meteorological Records: A Global Inventory, Bulletin of the American Meteorological Society, 100(12), pp.ES389-ES413, https://doi.org/10.1175/BAMS-D-19-0040.1, 2019a.

Brönnimann, S., Martius, O., Rohr, C., Bresch, D.N. and Lin, K.-H.E.: Historical weather data for climate risk assessment, Annals of the New York Academy of Sciences, 1436(1), pp.121-137, https://doi.org/10.1111/nyas.13966, 2019b.

Büntgen, U., Urban, O., Krusic, P.J. et al.: Recent European drought extremes beyond Common Era background variability, Nature Geoscience, 14(4), pp.190-196, https://doi.org/10.1038/s41561-021-00698-0, 2021.

Bürger, G.: On the verification of climate reconstructions, Climate of the Past, 3(3), pp.397-409, https://doi.org/10.5194/cp-3-397-2007, 2007.

Casty, C., Raible, C.C., Stocker, T.F. , Wanner, H. and Luterbacher, J.: A European pattern climatology 1766-2000, Climate Dynamics, 29(7-8), pp.791-805, https://doi.org/10.1007/s00382-007-0257-6, 2007.

https://doi.org/10.5194/egusphere-2026-3352
Preprint. Discussion started: 7 July 2026
© Author(s) 2026. CC BY 4.0 License.

Cook, E. R., et al. Old World megadroughts and pluvials during the Common Era. Science Advances, 1(10), e1500561, 10.1126/sciadv.1500561, 2015.

Coonan, B., Curley, M. and Ryan, C.: Long-term rainfall averages for Ireland 1991-2020, Climatological Note No.22, Met Éireann, https://www.edepositireland.ie/entities/publication/440059f6-bba8-4d7e-bb67-ea712d8c70ae, [Accessed 19 December 2025], 2024.

Cornes, R.C., Jones, P.D., Briffa, K.R. and Osborn, T.J.: A daily series of mean sea-level pressure for London, 1692-2007, International Journal of Climatology, 32(5), pp.641-656, https://doi.org/10.1002/joc.2301, 2012a.

Cornes, R.C., Jones, P.D., Briffa, K.R. and Osborn, T.J.: A daily series of mean sea-level pressure for Paris, 1670-2007, International Journal of Climatology, 32(8), pp.1135-1150, https://doi.org/10.1002/joc.2349, 2012b.

Cornes, R.C., Jones, P.D., Briffa, K.R. and Osborn, T.J.: Estimates of the North Atlantic Oscillation back to 1692 using a Paris-London westerly index, International Journal of Climatology, 33(1), pp.228-248, https://doi.org/10.1002/joc.3416, 2013.

Cornes, R.C., van der Schrier, G., van den Besselaar, E. J. M., and Jones, P.D.: An ensemble version of the E-OBS temperature and precipitation data sets, Journal of Geophysical Research: Atmospheres, 123(17), pp.9391-9409, https://doi.org/10.1029/2017JD028200, 2018.

Craddock, J.M. and Wales-Smith, B.G.: Monthly rainfall totals representing the East Midlands for the years 1726 to 1975, Meteorological Magazine, 106(4), pp.97-111, https://digital.nmla.metoffice.gov.uk/IO_8fc7172f-50f8-4792-b7e9-f972b3963adc/, [Accessed 26 December 2025], 1977.

Daly, C.: Guidelines for assessing the suitability of spatial climate data sets, International Journal of Climatology, 26(6), pp.707-721, https://doi.org/10.1002/joc.1322, 2006.

Daly, C., Doggett, M., Smith, J., Olson, K., Halbleib, M., Dimcovic, Z., Keon, D., Loiselle, R., Steinberg, B., Ryan, A., Pancake, C. and Kaspar, E.: Challenges in Observation-Based Mapping of Daily Precipitation across the Conterminous United States, Journal of Atmospheric and Oceanic Technology, 38(11), pp.1979-1992, https://doi.org/10.1175/JTECH-D-21-0054.1, 2021.

Dixon, F.E.: Weather in Old Dublin, Dublin Historical Record, 13(3-4), pp.94-107, https://www.jstor.org/stable/30103812, 1953.

Efron, B. and Tibshirani, R.J.: An Introduction to the Bootstrap, New York: Chapman and Hall, https://doi.org/10.1201/9780429246593, 1993.

Engler, S., Mauelshagen, F., Werner, J. and Luterbacher, J.: The Irish famine of 1740–1741: famine vulnerability and "climate migration", Climate of the Past, 9(3), pp.1161-1179, https://doi.org/10.5194/cp-9-1161-2013, 2013.

https://doi.org/10.5194/egusphere-2026-3352
Preprint. Discussion started: 7 July 2026
© Author(s) 2026. CC BY 4.0 License.

Fordham, S. and Murphy, C.: The Emergence of a Climate Change Signal in Ireland's Rainfall Extremes', *International Journal of Climatology*, 46(7), e70346, https://doi.org/10.1002/joc.70346, 2026.

Friedman, J. H., Hastie, T., and Tibshirani, R.: Regularization Paths for Generalized Linear Models via Coordinate Descent, Journal of Statistical Software, 33(1), pp.1-22, https://doi.org/10.18637/jss.v033.i01, 2010.

Gessler, A., Ferrio, J.P., Hommel, R., Treydte, K., Werner, R.A. and Monson, R.K.: Stable isotopes in tree rings: towards a mechanistic understanding of isotope fractionation and mixing processes from the leaves to the wood, Tree Physiology, 34(8), pp.796-818, https://doi.org/10.1093/treephys/tpu040, 2014.

Hastie, T., Tibshirani, R. and Friedman, J.: The Elements of Statistical Learning: Data Mining, Inference, and Prediction, 2nd edn., New York: Springer, https://doi.org/10.1007/978-0-387-84858-7, 2009.

Hawkins, E., Burt, S., McCarthy, M., Murphy, C., Ross, C., Baldock, M., Brazier, J., Hersee, G., Huntley, J., Meats, R., O'Grady, J., Scrimgeour, I. and Silk, T.: Millions of historical monthly rainfall observations taken in the UK and Ireland rescued by citizen scientists, Geoscience Data Journal, 10(2), pp.246-261, https://doi.org/10.1002/gdj3.157, 2023.

Herrera, S., Gutiérrez, J.M., Ancell, R., Pons, M.R., Frías, M.D. and Fernández, J.: Development and analysis of a 50-year high-resolution daily gridded precipitation dataset over Spain (Spain02), International Journal of Climatology, 32(1), pp.74-85, https://doi.org/10.1002/joc.2256, 2012.

Hofstra, N., Haylock, M., New, M. and Jones, P.D.: Testing E-OBS European high-resolution gridded data set of daily precipitation and surface temperature, Journal of Geophysical Research D: Atmospheres, 114(21), D21101, https://doi.org/10.1029/2009JD011799, 2009.

Horvath, C., Ryan, C., Murphy, C.: A Monthly Snow and Sleet Series for the Greater Dublin Area 1867-2024, Geoscience Data Journal, 12(4), e70022, https://doi.org/10.1002/gdj3.70022, 2025.

Hurrell, J.W.: Decadal trends in the North Atlantic Oscillation: regional temperatures and precipitation, Science, 269(5224), pp.676-679, 10.1126/science.269.5224.676, 1995.

Jenkinson, A.F., Shackleton, W. and Lawson, S.: Monthly and Annual Rainfall for Ireland, 1711-1977, Unpublished UK Met Office Branch Memorandum, No. 77, April 1979, 1979.

Jobbová, E., Crampsie, A., Murphy, C., Ludlow, F., McLeman, R., Horvath, C., Seifert, N., Myslinski, T., Sente, L.: The Irish drought impacts database: A 287-year database of drought impacts derived from newspaper archives, Geoscience Data Journal, 11(4), pp.1007-1023, https://doi.org/10.1002/gdj3.272, 2024.

Jones, P.D., Davies, T.D., Lister, D.H., Slonosky, V., Jónsson, T., Bärring, L., Jönsson, P., Maheras, P., Kolyva-Machera, F., Barriendos, M. and Martin-Vide, J.: Monthly mean pressure reconstructions for Europe for the 1780–1995 period, International Journal of

https://doi.org/10.5194/egusphere-2026-3352
Preprint. Discussion started: 7 July 2026
© Author(s) 2026. CC BY 4.0 License.

Climatology, 19(4), pp.347–364, https://doi.org/10.1002/(SICI)1097-0088(19990330)19:4<347::AID-JOC363>3.0.CO;2-S, 1999.

Jones, P.D., Jónsson, T. and Wheeler, D.: Extension to the North Atlantic Oscillation using early instrumental pressure observations from Gibraltar and south-west Iceland, International Journal of Climatology, 17(13), pp.1433-1450, https://doi.org/10.1002/(SICI)1097-0088(19971115)17:13<1433::AID-JOC203>3.0.CO;2-P, 1997.

Jones, P.D., Wigley, T.M.L. and Briffa, K.R.: Monthly Mean Pressure Reconstructions for Europe (back to 1780) and North America (to 1858), Technical Note TR037, Washington, DC: U.S. Department of Energy, 1987.

Kelly-Quinn, M., Blacklocke, S., Bruen, M., Earle, R., O'Neill, E., O'Sullivan, J. and Purcell, P.: Dublin Ireland: a city addressing challenging water supply, management, and governance issues, Ecology and Society, 19(4), 10, http://dx.doi.org/10.575, 2014.

Kendon, L., Short, C., Cotterill, D., Pirret, J., Chan, S. and Pope, J.: UK Climate Projections: UKCP Local (2.2km) Transient Projections, Met Office, https://www.metoffice.gov.uk/binaries/content/assets/metofficegovuk/pdf/research/ukcp/ukcp_local_report_2023.pdf, [Accessed 19 December 2025], 2023.

Klesse, S., Weigt, R., Treydte, K., Saurer, M., Schmid, L., Siegwolf, R.T.W., Frank, D.C.: Oxygen isotopes in tree rings are less sensitive to changes in tree size and relative canopy position than carbon isotopes, Plant, Cell and Environment, 41(12), pp.2899-2914, 10.1111/pce.13424, 2018.

Li, J., Pollinger, F., and Paeth, H.: Comparing the Lasso Predictor-Selection and Regression Method with Classical Approaches of Precipitation Bias Adjustment in Decadal Climate Predictions, Monthly Weather Review, 148(10), pp.4339-4351, https://doi.org/10.1175/MWR-D-19-0302.1, 2020.

Liaw, A. and Wiener, M.: Classification and Regression by randomForest, R News, 2(3), pp.18-22, https://journal.r-project.org/articles/RN-2002-022/RN-2002-022.pdf, [Accessed 30 December 2025], 2002.

Loader, N.J., Mccarroll, D., Miles, D., Young, G.H.F., Davies, D. and Ramsey, C.B.: Tree ring dating using oxygen isotopes: a master chronology for central England, Journal of Quaternary Science, 34(6), pp.475-490, https://doi.org/10.1002/jqs.3115, 2019.

Loader, N.J., Young, G.H.F., McCarroll, D., Davies, D., Miles, D., and Bronk Ramsey, C.: Summer precipitation for the England and Wales region, 1201-2000 CE, from stable oxygen isotopes in oak tree rings, Journal of Quaternary Science, 35(6), pp.731-736, https://doi.org/10.1002/jqs.3226, 2020.

Luterbacher, J., Schmutz, C., Gyalistras, D., Xoplaki, E. and Wanner, H.: Reconstruction back to AD 1675 of monthly NAO and EU indices, Geophysical Research Letters, 26(17), pp.2745-2748, https://doi.org/10.1029/1999GL900576, 1999.

https://doi.org/10.5194/egusphere-2026-3352
Preprint. Discussion started: 7 July 2026
© Author(s) 2026. CC BY 4.0 License.

Luterbacher, J., Xoplaki, E., Dietrich, D., Rickli, R., Jacobeit, J., Beck, C., Gyalistras, D., Schmutz, C. and Wanner, H.: Reconstruction of sea level pressure fields over the Eastern North Atlantic and Europe back to 1500, Climate Dynamics, 18, pp.545-561, https://doi.org/10.1007/s00382-001-0196-6, 2002.

Manley, G.: Snowfall in Britain over the past 300 years, Weather, 24(11), pp.428–437, https://doi.org/10.1002/j.1477-8696.1969.tb03117.x, 1969.

Manley, G.: Central England temperatures: Monthly means 1659 to 1973, Quarterly Journal of Royal Meteorological Society, 100(425), pp.389-405, https://doi.org/10.1002/qj.49710042511, 1974.

Matiu, M., Napoli, A., Kotlarski, S. Zardi, D., Bellin, A. and Majone, B.: Elevation-dependent biases of raw and bias-adjusted EURO-CORDEX regional climate models in the European Alps,. Climate Dynamics, 62(10), pp.9013-9030, https://doi.org/10.1007/s00382-024-07376-y, 2024.

McCarroll, D. and Loader, N.J.: Stable isotopes in tree rings, Quaternary Science Reviews, 23(7-8), pp.771-801, https://doi.org/10.1016/j.quascirev.2003.06.017, 2004.

Murphy, C., Broderick, C., Burt, T. P., Curley, M., Duffy, C., Hall, J., Harrigan, S., Matthews, T. K. R., Macdonald, N., McCarthy, G., McCarthy, M. P., Mullan, D., Noone, S., Osborn, T. J., Ryan, C., Sweeney, J., Thorne, P. W., Walsh, S., and Wilby, R. L.: A 305-year continuous monthly rainfall series for the island of Ireland (1711-2016), Climate of the Past, 14(3), pp.413-440, https://doi.org/10.5194/cp-14-413-2018, 2018.

Murphy, C., Wilby, R.L., Matthews, T., Horvath, C., Crampsie, A., Ludlow, F., Noone, S., Brannigan, S., Hannaford, J., McLeman, R., Jobbova, E.: The forgotten drought of 1765-1768: Reconstructing and re-evaluating historical droughts in the British and Irish Isles, International Journal of Climatology, 40(12), pp.5329-5351, https://doi.org/10.1002/joc.6521, 2020.

Murphy, C., Wilby, R.L., Matthews, T.K.R., Thorne, P., Broderick, C., Fealy, R., Hall, J., Harrigan, S., Jones, P., McCarthy, G., MacDonald, N., Noone, S. and Ryan, C.: Multi-century trends to wetter winters and drier summers in the England and Wales precipitation series explained by observational and sampling bias in early records, International Journal of Climatology, 40(1), pp.610-619, https://doi.org/10.1002/joc.6208, 2019.

Newman, A., Clark, M., Craig, J., Nijssen, B., Wood, A., Gutmann, E., Mizukami, N., Brekke, L. and Arnold, J.: Gridded Ensemble Precipitation and Temperature Estimates for the Contiguous United States, Journal of Hydrometeorology, 16(6), pp. 2481-2500, https://doi.org/10.1175/JHM-D-15-0026.1, 2015.

Noone, S., Murphy, C., Coll, J., Matthews, T., Mullan, D., Wilby, R.L. and Walsh, S.: Homogenization and analysis of an expanded long-term monthly rainfall network for the Island of Ireland (1850-2010), International Journal of Climatology, 36(8), pp.2837-2853, https://doi.org/10.1002/joc.4522, 2016.

https://doi.org/10.5194/egusphere-2026-3352
Preprint. Discussion started: 7 July 2026
© Author(s) 2026. CC BY 4.0 License.

Noone, S., Broderick, C., Duffy, C., Matthews, T., Wilby, R.L. and Murphy, C.: A 250-year drought catalogue for the island of Ireland (1765-2015), International Journal of Climatology, 37(S1), pp.239-254, https://doi.org/10.1002/joc.4999, 2017.

O'Connor, P., Murphy, C., Matthews, T. and Wilby, R..: Reconstructed monthly river flows for Irish catchments 1766-2016, Geoscience Data Journal, 8(1), pp.34-54, https://doi.org/10.1002/gdj3.107, 2021.

Parker, D.E., Legg, T.P. and Folland, C.K.: A new daily central England temperature series, 1772-1991, International Journal of Climatology, 12(4), pp.317-342, https://doi.org/10.1002/joc.3370120402, 1992.

Parry, S.; Lavers, D., Wilby, R., Prudhomme, C., Wood, P., Murphy, C. and O'Connor, P.: Abrupt drought termination in the British-Irish Isles driven by high atmospheric vapour transport, Environmental Research Letters, 18(10), 104050, 10.1088/1748-9326/acf145 , 2023.

Pauling, A., Luterbacher, J., Casty, C. and Wanner, H.: Five hundred years of gridded high-resolution precipitation reconstructions over Europe and the connection to large-scale circulation, Climate Dynamics, 26, pp.387-405, https://doi.org/10.1007/s00382-005-0090-8, 2006.

Peña-Angulo, D., Vicente-Serrano, S. M., Domínguez-Castro, F., Lorenzo-Lacruz, J., Murphy, C., Hannaford, J., Allan, R.P., Tramblay, Y., Reig-Garcia, F. and El Kenway, A.: The complex and spatially diverse patterns of hydrological droughts across Europe, Water Resources Research, 58(4), e2022WR031976, https://doi.org/10.1029/2022WR031976, 2022.

Pollock, M.D., O'Donnell, G., Quinn, P., Dutton, M., Black, A., Wilkinson, M.E., Colli, M., Stagnaro, M., Lanza, L.G., Lewis, E., Kilsby, C.G. and O'Connel, P.E.: Quantifying and mitigating wind-induced undercatch in rainfall measurements, Water Resources Research, 54(6), pp.3863-3875, https://doi.org/10.1029/2017WR022421, 2018.

Rogers, J. C.: The Association between the North Atlantic Oscillation and the Southern Oscillation in the Northern Hemisphere, Monthly Weather Review, 112(10), pp.1999-2015, https://doi.org/10.1175/1520-0493(1984)112<1999:TABTNA>2.0.CO;2, 1984.

Rudd, A.C., Bell, V.A. and Kay, A.L.: National-scale analysis of simulated hydrological droughts (1891–2015), Journal of Hydrology, 550, pp.368-385, 10.1016/j.jhydrol.2017.05.018, 2017.

Rutty, J.: A Chronological History of the Weather and Seasons, and of the Prevailing Diseases in Dublin: With Their Various Periods, Successions, and Revolutions, During the Space of Forty Years With a Comparative View of the Difference of the Irish Climate and Diseases, and Those of England and Other Countries, Robinson and Roberts, London: 1770, 1770.

https://doi.org/10.5194/egusphere-2026-3352
Preprint. Discussion started: 7 July 2026
© Author(s) 2026. CC BY 4.0 License.

Ryan, C., Curley, M., Walsh, S. and Murphy, C.: Long-term trends in extreme precipitation indices in Ireland, International Journal of Climatology, *42*(7), pp.4040-4061, https://doi.org/10.1002/joc.7475, 2022.

Ryan, C. and McGovern, R.: Irish Weather Rescue Project, Met Éireann, https://www.zooniverse.org/projects/met-rhonda/irish-weather-rescue, [Accessed 18 December 2025], 2025.

Ryan, C., Murphy, C., McGovern, R., Curley, M., Walsh, S. and 476 students: Irelands pre-1940 daily rainfall records, Geoscience Data Journal, 8(1), pp.11-23, https://doi.org/10.1002/gdj3.103, 2021.

Shields L.: The beginnings of scientific weather observation in Ireland (1684-1708), Weather, 38(10), pp.304-311, https://doi.org/10.1002/j.1477-8696.1983.tb04811.x, 1983.

Strangeways, I.C.: Back to basics: The met. enclosure Part 2(b) - Rain gauges, their errors, Weather, 51(9), pp.298-303, https://doi.org/10.1002/j.1477-8696.1996.tb06230.x, 1996.

Strangeways, I.: A history of rain gauges, Weather, 65(5), pp.133-138, https://doi.org/10.1002/wea.548, 2010.

Tabony, R.C.: A revised rainfall series for Spalding, Lincolnshire, Meteorological Magazine, 109(1294), pp.152-157, https://digital.nmla.metoffice.gov.uk/IO_97b1364d-379d-4fe0-bf1f-87b52ff69af3/, [Accessed 26 December 2025], 1980.

Tetko, I.V., Livingstone, D.J., and Luik, A.I.: Neural network studies. 1. Comparison of overfitting and overtraining, Journal of Chemical Information and Computer Sciences, 35(5), pp.826-833, https://doi.org/10.1021/ci00027a006, 1995.

Tibshirani, R.: Regression Shrinkage and Selection Via the Lasso, Journal of the Royal Statistical Society: Series B (Methodological), 58(1), pp.267-288, https://doi.org/10.1111/j.2517-6161.1996.tb02080.x, 1996.

Todd, B., Macdonald, N., Chiverrell, R.C., Caminade, C., and Hooke, J.M.: Severity, duration and frequency of drought in SE England from 1697-2011, Climatic Change, 121(4), pp.673-687, https://doi.org/10.1007/s10584-013-0970-6, 2013.

Uisce Éireann: Regional Water Resources Plan-Eastern and Midlands Non-Technical Summary, Uisce Éireann, https://www.water.ie/sites/default/files/docs/rwrp-easternmidlands/2022/rwrp-em-nts/RWRP-EM-NTS.pdf, [Accessed 09 January 2026], 2022a.

Uisce Éireann: Regional Water Resources Plan- Eastern and Midlands Study Area 9 Technical Report, Uisce Éireann, https://www.water.ie/sites/default/files/projects/strategic-plans/national-water-resources/rwrp/eastern-midlands/RWRP-EM-Appendix-9-Study-Area-9-Technical-Report.pdf?utm_source=chatgpt.com, [Accessed 16 October 2025], 2022b.

Wales-Smith, B.G.: Monthly and annual totals of rainfall representative of Kew, Surrey, from 1697 to 1970, Meteorological Magazine, 100(1193), pp.345-360,

https://doi.org/10.5194/egusphere-2026-3352
Preprint. Discussion started: 7 July 2026
© Author(s) 2026. CC BY 4.0 License.

https://digital.nmla.metoffice.gov.uk/IO_e22505c4-c460-4833-8d3c-b0146537ab0e/ [Accessed 26 December 2025], 1971.

Wetter, O., Pfister, C., Werner, J.P. et al.: The year-long unprecedented European heat and drought of 1540 - a worst case. Climatic Change, 125 (3-4), pp.349-363, https://doi.org/10.1007/s10584-014-1184-2, 2014.

Wilby, R.L. and Murphy, C.: Decision-making by water managers despite climate uncertainty, In: Pfeffer, W.T., Smith, J.B. and Ebi, K.L. (Eds) The Oxford Handbook of Planning for Climate Change Hazards, Oxford: Oxford University Press, https://doi.org/10.1093/oxfordhb/9780190455811.013.52, 2019.

Wilby, R.L., O'Hare, G. and Barnsley, N.: The North Atlantic Oscillation and British Isles climate variability, 1865-1996, Weather, 52(9), pp.266-276, https://doi.org/10.1002/j.1477-8696.1997.tb06323.x, 1997.

Wilby R., Prudhomme, C., Parry, S. and Muchan, K.G.L.: Persistence of Hydrometeorological Droughts in the United Kingdom: A Regional Analysis of Multi-Season Rainfall and River Flow Anomalies, Journal of Extreme Events, 2(2), 1550006, https://doi.org/10.1142/S2345737615500062, 2015.